

MARIA S. MERIAN-Berichte

**BalTec**

Cruise No. MSM52

1.3.-28.3.2016,  
Rostock (Germany) – Kiel (Germany)

MSM52



BalTec

Christian Hübscher, Niklas Ahlrichs, Gareth Allum, Thomas Behrens, Joachim Bülow, Charlotte Krawczyk, Volkmar Damm, Ümit Demir, Martin Engels, Laura Frahm, Jarosław Grzyb, Boris Hahn, Ingo Heyde, Chris Juhlin, Katharina Knevels, Gerhard Lange, Ida Bruun Lydersen, Gerhard Lange, Michal Malinowski, Vera Noack, Jonas Preine, Keygan Rampersad, Michael Schnabel, Elisabeth Seidel, Daniel Sopher, Janne Marie Stakemann, Josefine Stakemann

Editorial Assistance:

DFG-Senatskommission für Ozeanographie  
MARUM – Zentrum für Marine Umweltwissenschaften der Universität Bremen

## Table of Contents

	Page
1 Summary	4
2 Participants	5
3 Research Program	7
3.1 Setting	7
3.2 Scientific Aims	11
3.2.1 Ice-Load Induced Tectonics	11
3.2.2 Salt Tectonics and Fluids	11
3.2.3 Other Upcoming Objectives	12
3.3 Survey Layout	13
3.4 Relevance of the Seismic Survey to BGR's Project "TUNB"	14
3.5 Marine Mammal Observation to Comply With Environmental Best Practice Standards	15
3.5.1 General Remarks	15
3.5.2 Conventional Visual Observations	17
3.5.3 Conventional Passive Acoustic Monitoring PAM	18
3.5.4 QuietSea System for Passive Acoustic Monitoring	19
3.5.5 Conclusions Regarding Mitigation & Compliance with JNCC Guidelines	20
4 Narrative of the Cruise	21
5 Preliminary Results	22
5.1 Processing of MCS Data	22
5.1.1 Geometry Setup	22
5.1.2 Pre-Processing	24
5.1.3 Velocity Analysis	25
5.1.4 Multiple Elimination	26
5.1.5 Stacking and Migration	26
5.1.6 Post-Processing	26
5.2 Wide-Angle Reflection Refraction Seismics	27
5.3 Hydroacoustics	30
5.4 Gravimetry	31
5.4.1 Sea Gravimeter System KSS31	31
5.4.2 Gravity Ties to Land Stations	31
5.4.3 Gravity Data Processing	35
5.5 Expected Results	35
5.5.1 Reflection Seismics	35
5.5.2 Streamer Refractions	37
5.5.3.OBS Recordings	39
5.6.4 Gravity Data	41
6 Station List MSM52	42
7 Data and Sample Storage and Availability	46
8 Acknowledgements	46
9 References	47

10	Appendix	49
	10.1 Seismic Equipment and Survey Setup	49

## 1 Summary

(C. Hübscher)

The major pre-alpine tectonic lineaments as the Glückstadt Graben and the Avalonia-Baltica suture zone run across the southern Baltic. The BalTec-expedition aimed at the gapless imaging of these fault systems from the seafloor down to the Paleozoic basement. Scientifically the expedition was motivated by two hypotheses. We postulated that advances and retreats of ice-sheets during the glacials initiated and reactivated faulting of the Post-Permian succession, thereby generating several kilometers long near-vertical faults and anticlines. We further postulated that – in contrast to the generally accepted text book models – deformation of the initially up to 1800 m thick Zechstein salt started already during salt deposition as the consequence of salt load induced basin subsidence and resulting salt creep. The profile network was further designed to allow for linking the stratigraphy between previously generated local underground models in the frame of the TUNB project. Altogether we collected 62 reflection seismic profiles of an entire length of 3500 km. Parasound and multibeam data were collected along 6000 km each. The marine gravimeter collected data along the entire ship's track of 7000 km. Two wide-angle reflection / refraction profiles have been measured in order to image the deep structure of the Teisseyre-Tornquist Zone off Poland and to investigate North-South striking fault systems in the Bay of Kiel. The JNCC (2010) 'Guidelines for minimising the risk of injury and disturbance to marine mammals from seismic surveys' were followed throughout the survey.

*Im Untergrund der südlichen Ostsee verlaufen die dominierenden prä-alpinen Störungssysteme Nordeuropas, z.B. der Glückstadtgraben und die Avalonia-Baltica Suturezone. Arbeitsziele des BalTec-Projektes waren, diese Störungssysteme lückenlos vom Meeresboden bis zum paläozoischen Grundgebirge mit bisher unerreichter Auflösung reflexions- und refraktionsseismisch abzubilden. Überprüft werden sollte die These, dass das Vor- und Zurückschreiten der Eisgletscher während der Eiszeiten in den post-permischen Abfolgen Bruchtektonik initiierte und zuvor angelegte Störungen reaktivierte. Diese glazial induzierte Tektonik erzeugte über viele Kilometer lange, steil-stehende Störungen und Antiklinen. Weiterhin galt es die Frage zu untersuchen, ob entgegen der Lehrbuch-Modelle die Deformation der initial bis zu 1800 m mächtigen Zechsteinabfolgen bereits während der Salzablagerung erfolgte. Die These lautet, dass die größer werdende Salzauflast zu Subsidenz und Verkipfung des Beckens führte, was wiederum Salzfluss zum Subsidenzzentrum veranlasste. Die Profile wurden außerdem so geplant, dass mit ihnen im Rahmen des TUNB-Projektes die stratigraphische Verbindung zwischen bestehenden, lokalen Untergrundmodellen hergestellt werden kann. Insgesamt vermaßen wir 62 reflexionsseismische Profile mit einer Gesamtlänge von etwa 3500 km. Parasound und Fächerlotdaten wurden über eine Strecke von ca. 6000 km aufgezeichnet. Das Gravimeter zeichnete Schweredaten entlang der gesamten Fahrtroute von etwa 7000 km auf. Bei den beiden Weitwinkelprofilen über die Teisseyre-Tornquist Zone entlang der polnischen Küste sowie über die Nord-Süd streichenden Störungssysteme in der Kieler Bucht kamen 15 bzw. 10 OBS zum Einsatz. Während der Ausfahrt wurden die JNCC (2010) 'Guidelines for minimising the risk of injury and disturbance to marine mammals from seismic surveys' konsequent angewendet.*

## 2 Participants

Name	Discipline	Institution
Prof. Dr. Hübscher, Christian	Marine Geophysics / Chief Scientist	IfG / CEN
Ahlich, Niklas	Marine Geophysics	IfG / CEN
Bülow, Joachim	Marine Geophysics	IfG / CEN
Frahm, Laura	Marine Geophysics	IfG / CEN
Stakemann, Janne Marie	Marine Geophysics	IfG / CEN
Knevels, Katharina	Marine Geophysics	IfG / CEN
Preine, Jonas	Marine Geophysics	IfG / CEN
Stakemann, Josefine	Marine Geophysics	IfG / CEN
Dr. Damm, Volkmar	Marine Geophysics	BGR
Behrens, Thomas	Marine Geophysics	BGR
Demir, Ümit	Marine Geophysics	BGR
Hahn, Boris	Marine Geophysics	BGR
Lange Gerhard	Marine Geophysics	BGR
Dr. Noack, Vera	Marine Geophysics	BGR (Berlin)
Dr. Schnabel, Michael	Marine Geophysics	BGR
Dr. Engels, Martin	Marine Geophysics	BGR
Seidel, Elisabeth	Marine Geophysics	IGG-EMA
Prof. Dr. Malinowski, Michal	Marine Geophysics	IGF-PAS
Grzyb, Jarosław	Marine Geophysics	IGF-PAS
Lydersen, Ida Bruun	Marine Geophysics	DES-UU
Allum, Gareth	Marine Mammal Observer	MSeis
Rampersad, Keygan	Technical Support	SERCEL

Onshore Team: (Add Tomasz, Obst, Meschede)

Name	Discipline	Institution
Prof. Dr. Chris Juhlin	Marine Geophysics	DES-UU
Dr. Ingo Heyde	Marine Geophysics	BGR
Prof. Dr. Charlotte Krawczyk	Geophysics	GFZ
Dr. Daniel Sopher	Marine Geophysics	DES-UU

### BGR

Bundesanstalt für Geowissenschaften und  
Rohstoffe  
Federal Institute for Geosciences and  
Natural Resources  
Stilleweg 2  
30655 Hannover/ Germany  
www.bgr.bund.de

### BGR (Berlin)

Bundesanstalt für Geowissenschaften und  
Rohstoffe  
Federal Institute for Geosciences and  
Natural Resources  
Dienstbereich Berlin  
Wilhelmstrasse 25 - 30

13593 Berlin / Germany

[www.bgr.bund.de](http://www.bgr.bund.de)

**DES-UU**

Department of Earth Sciences

Uppsala University

Geocentrum, Villav. 16

752 36 Uppsala / Sweden

[katalog.uu.se/orginfo/?orgId=X35:4](http://katalog.uu.se/orginfo/?orgId=X35:4)

**GFZ**

GFZ German Research Centre for  
Geosciences

Telegrafenberg

14473 Potsdam

<http://www.gfz-potsdam.de>

**IFG / CEN**

Institut für Geophysik

Centrum für Erdsystemforschung und  
Nachhaltigkeit

Universität Hamburg

Bundesstraße 55

20146 Hamburg / Germany

[www.geo.uni-hamburg.de/geophysik/](http://www.geo.uni-hamburg.de/geophysik/)

**IGF-PAS**

Institute of Geophysics

Polish Academy of Sciences

Department of the Lithospheric Research

Ks. Janusza 64

01-452 Warsaw / Poland

**IGG-EMA**

Institut für Geographie und Geologie

Ernst Moritz Arndt Universität Greifswald

Friedrich-Ludwig-Jahn-Str. 17A

17487 Greifswald / Germany

[www.mnf.uni-](http://www.mnf.uni-greifswald.de/institute/geo.html)

[greifswald.de/institute/geo.html](http://www.mnf.uni-greifswald.de/institute/geo.html)

**MSeis**

43A Sandford Road, Weston-super-Mare

Somerset, BS23 3EX / UK

**SERCEL**

17200 Park Row

Houston

Texas 77084 / USA

[www.sercel.com](http://www.sercel.com)

### 3 Research Program

#### 3.1 Setting

(C. Hübscher, V. Damm, C. Juhlin, C. Krawczyk, M. Malinowski, V. Noack, E. Seidel)

*Plate tectonics:* As summarized by Maystrenko et al. (2005) East Avalonia accreted to Baltica during the Late Ordovician-earliest Silurian, causing the formation of the Caledonian Deformation Front (Fig. 3.1.1) which is documented by seismic lines as a zone of thrusting (e.g., Abramovitz et al. 1998; Krawczyk et al. 2002). This collision between Avalonia and Baltica marked the last stage of Laurussia suturing. Since the 1990s, the Thor Suture (or Caledonian Deformation Front at the shallow level) has usually been considered as the collision suture between Baltica and East Avalonia (Pharaoh et al. 1997) while Cocks et al. (1997) preferred the Elbe-Odra Line as the major contact zone. These opposing theses and all available data at that time are reviewed in Krawczyk et al. (2008a). They show that the faults closest to the surface rather project at the CDF, while the high-velocity Baltica crust runs out below the North-German Basin as a wedge-shaped feature ending immediately north of the Elbe line.

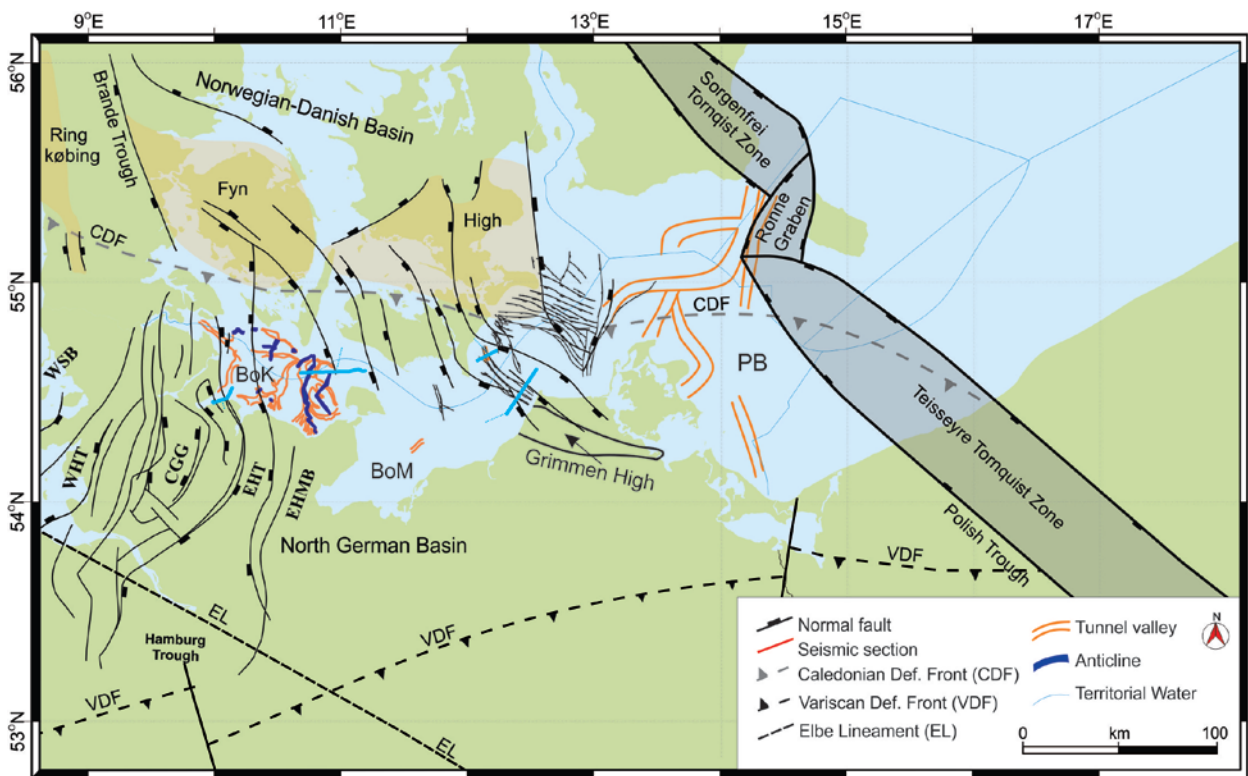


**Fig. 3.1.1** Study area with main structural elements (compiled from Baldschuhn et al., 1991; Krauss, 1994; Vejrbæk, 1997; Bayer et al., 1999; Clausen and Pedersen, 1999; Kossow et al., 2000). BoK, Bay of Kiel; BoM, Bay of Mecklenburg; EHMB, Eastholstein Mecklenburg Block; EHT, Eastholstein Trough; CGG, Central Glückstadt Graben; PB, Pomeranian Bay; WHT, Westholstein Trough.

*North German Basin:* The North German Basin (Fig. 3.1.1), which is a sub-basin of the Southern Permian Basin (Ziegler, 1990; Scheck and Bayer, 1999), belongs to a series of related Carboniferous-Permian intra-continental basins extending from the southern North Sea to

Northern Poland (Kossow et al., 2000), referred to as the Central European Basin System. The Ringkøbing-Fyn High is a series of east-west striking basement highs running across the North Sea and the Danish mainland (Clausen and Pedersen, 1999) that bounds the North German Basin to the north. The southern flank of the Ringkøbing-Fyn High is more or less identical to the path of the Caledonian Deformation Front. To the south, the North German Basin terminates at the Variscan Deformation Front and to the east at the Teisseyre-Tornquist Zone.

The Glückstadt Graben represents a NNE–SSW trending post-Permian sub-basin of the CEBS (Maystrenko et al., 2005). The Glückstadt Graben is one of the sedimentary basins where the sedimentary cover has been strongly affected by salt tectonics. The onset of the regional E–W directed extension at the transition between the Middle and Late Triassic created N–S trending depocentres, as well as the associated salt structures, such as the Glückstadt Graben. The eastern SW–NE trending marginal Eastholstein Trough evolved during the Jurassic period (Maystrenko et al., 2011).

*Tornquist Fan:* A summary of the Tornquist Fan is given by Thybo (2000). The Tornquist Zone region occupies the northwestern part of the Trans European Suture Zone, which is the area of Palaeozoic amalgamation of the crust and lithosphere of Central Europe onto the Proterozoic Baltic Shield and East European Platform (Pharaoh & TESZ Colleagues 1996, Thybo et al., 1999). The Tornquist Fan proper comprises the area between the Fennoscandian Border Zone and the Trans European Fault and incorporates other fault zones in between (Fig. 3.2.1). The Tornquist Fan is a post-collisional feature, which formed as a northwestwards widening splay of faults during late Palaeozoic rifting of the region which also initiated wide-spread basin formation and general subsidence at the southwestern corner of the former Baltica plate (Thybo & Berthelsen 1991, Berthelsen 1992, Thybo 1997) (Fig. 3.1.1). Its reactivation is proposed to have started contemporaneously with the Pyrenean orogeny in late Cretaceous when Africa's SSE-directed sinistral transform motion relative to Europe changed to NE-directed convergence (Kley & Vogt, 2008). The Grimmen High that stretches from Darss to south of Rügen has been interpreted as a drag-related salt anticline at the margin of the North-East German Basin that developed in a transpressional setting (Kossow et al., 2000, Hübscher et al., 2010).

*Ice-load induced tectonics:* The large scale interaction between ice-sheet loading and unloading and lithosphere flexure as well as Pleistocene glacial features like moraines or tunnel valleys is well understood (see overview by Lang et al., 2014 and references therein). As suggested by Sirocko et al. (2008) (Fig. 3.1.2) and Al-Hseinat et al. (2016) and based on numerical studies Lang et al. (2014) concluded that ice-sheet loading on top of a salt diapir forces the diapir to move downwards. Reversal salt flow occurs after ice-sheet retreat and most of the downward displacement is compensated. If the ice-sheet remains outside the diapir, the load on the source layer causes the salt to flow into the diapir and the diapir rises. Al-Hseinat and Hübscher (2014) related near-vertical faults and elongated anticlines in the SW Baltic Sea to ice-load tectonics. The authors suggested that most of the faults that reach up to the seafloor into the Quaternary / Holocene sediment cover result from ice-load induced tectonics.

*Salt Tectonics:* Salt diapirism and salt pillow growth in the study area has been intensely studied by means of high-resolution seismics by Hansen et al. (2005; 2007), Hübscher et al. (2004; 2010) and Zöllner et al. (2008). Halokinesis could be related to the Triassic W-E extension, Jurassic North Sea doming, opening of the Atlantic and the Alpine orogeny. Onshore, Kossow et al. (2000) concluded that salt tectonics was initiated in the Late Jurassic / Early Cretaceous.



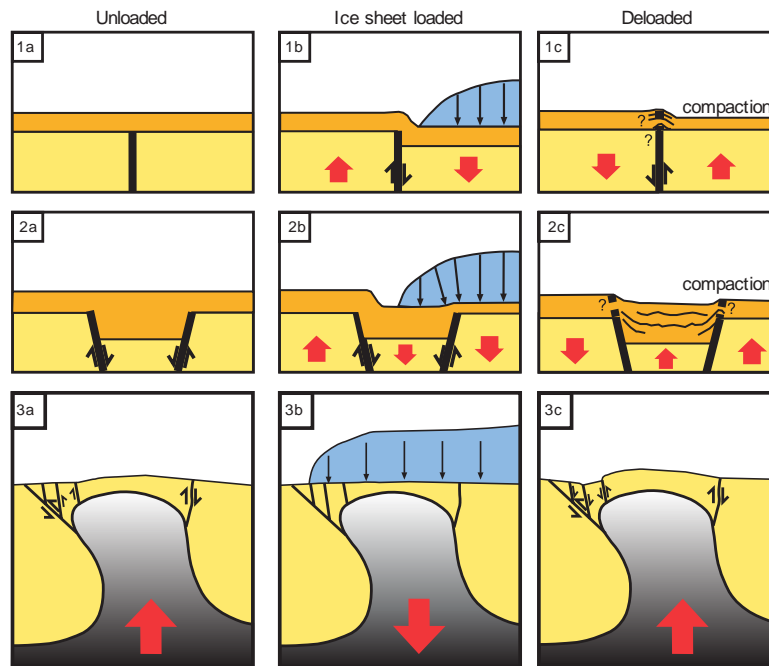


**Fig. 3.1.2** Ice load induced tectonism (from Sirocko et al., 2008). 1a-c) Influence of ice-loading/unloading on a normal fault with crustal failure and reactivation of inherited structures. Red arrows indicate relative crustal movements. 2a-c) Effects of ice-loading/unloading on a pre-existing graben system with conjugate faults. 3a-c) Consequences of ice-loading/unloading on faults and salt dynamics associated with a salt diapir, red arrows indicate relative diapiric movements.

Generally, salt tectonics produces some of the most complex low-temperature geological deformation seen on the earth surface, deep within sedimentary basins and on continental margins (Warren, 2008). According to paradigms which are nowadays generally accepted accommodation space for a rising diapir is created by thin-skinned extension (Vendeville and Jackson, 1992, Mohr et al., 2005). Vice versa, phases of reactive diapirism have been considered as indicators to conclude on plate tectonic pulses (e.g., Mohr et al., 2007). This initial creation of accommodation space by thin-skinned extension is the weak point of this conceptual model, since the created accommodation space above a future diapir needs a width of some kilometers.

When the weight of the fault blocks is equal or beneath the pressure within the salt, the salt will rise (*reactive diapirism*) (Fig. 3.1.3). If the overburden is thinned to less than 10% in thickness of the salt buoyancy forces further growth (*active diapirism*). Once a diapir has reached the surface, its top will remain at or close to the surface. The differential sediment load in the rim synclines squeezes the salt from the tabular reservoir into the diapir (*passive diapirism*). Diapirism stops if the reservoir is depleted.

Faulting in the sub-salt usually results in delocalized faulting in the supra-salt domain (Warren, 2008). The diapir that evolved above the fault during reactive, active and passive diapirism may growth further during inversion.

This concept was advanced by numerous studies of the Messinian salt in the Levant Basin in the easternmost Mediterranean (for summaries see Hübscher and Netzeband, 2007; Gvirtzman et al., 2013; Reiche et al., 2014 and references therein). It was concluded that deformation of a salt giant starts already during the precipitation and deposition of the salt. Salt deposition causes basin

subsidence and as the consequence the emerging salt layer creeps towards the basin center causing internal folding and thrusting (“gravity gliding”). The thickness variations of the salt are considered to be significant enough that sedimentation in the depressions directly initiate differential load and passive diapirism.

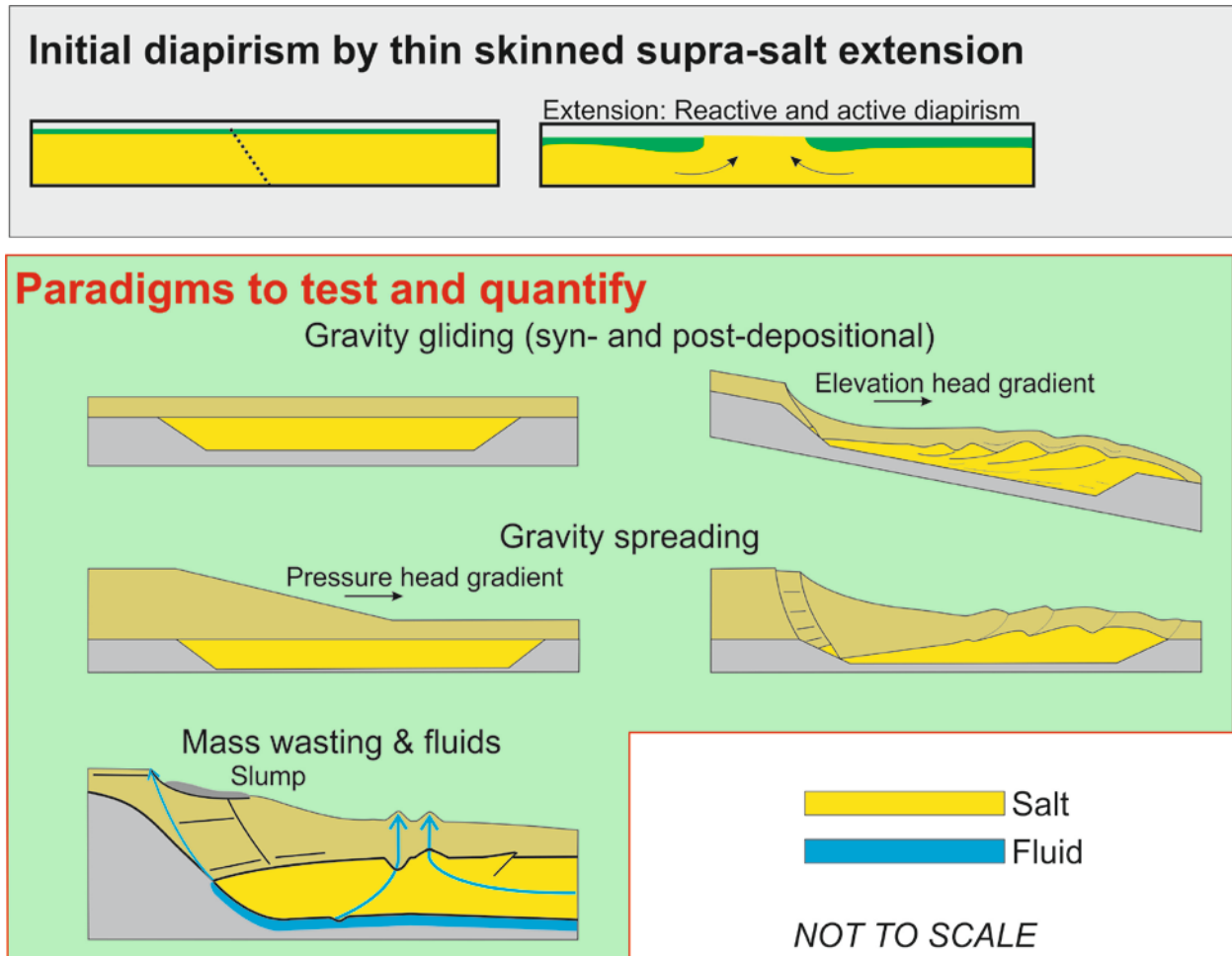


**Fig. 3.1.3** Compilation of conceptual models to explain syn- and post-depositional salt tectonics. This proposal is motivated by the hypothesis that the gravity gliding and gravity spreading approach can substitute the rather vaguely described reactive and active diapirism concept in tectonically stable basins.

Validating this assumption for the Zechstein salt in the Northeast German Basin would result in a paradigm shift, since the concepts of reactive diapirism, which occur in an extensive setting and represent precursors of passive diapirism, are no longer needed.

For instance, the enigmatic tectonic pulse proposed by Mohr et al. (2007) is no longer needed to explain salt tectonic initiation, if this new hypothesis holds. Another end-member model which is discussed for the Levant Basin is “gravity spreading”. According to this model the differential load caused by basin ward prograding sediment prisms squeeze the salt forward. It is a reasonable assumption that both processes, gravity gliding and gravity spreading, combine to deform the salt body during this stage.

A fundamental observation in Eastern Mediterranean Levant Basin seismic record is focussed fluid flow through and out of a several hundred meter thick tabular salt body causing circular

dissolution structures at the top of salt and mud volcanoes at the seafloor to where fluids that escaped from the salt deliver remobilized sediments (Gradmann et al., 2005; Bertoni and Cartwright, 2006; Netzeband et al., 2006; Hübscher and Dümmong, 2011). Such observations counter the general assumption that massive salt layers represent stratigraphic seals. Validating this observation would have enormous consequences for the understanding of thermal and chemical evolution of salt-floored basins.

### 3.2 Scientific Aims

(C. Hübscher, V. Damm, C. Juhlin, C. Krawczyk, M. Malinowski, V. Noack, E. Seidel)

The proposal is driven by two working hypotheses:

- 1) Ice-sheet loading and unloading initiates or reactivates faulting.
- 2) Deformation of the Zechstein salt started during salt deposition.

#### 3.2.1 Ice-load induced tectonics

In accordance to the conceptual models of Sirocko et al. (2008) and as proposed by Al-Hseinat and Hübscher (2014) or Al-Hseinat et al. (2016) the abundant near vertical faults and anticlines in the Post-Permian strata of the SW-Baltic are the consequence of ice-load induced tectonics. Al-Hseinat and Hübscher (2014) postulated reactivation of sub-salt faults, Lang et al. (2014) suggested that neotectonics above salt diapirs can result from thin-skinned salt tectonics. Two fundamental questions are:

- Is the supra-salt faulting the consequence of ice-load induced reactivation of sub-salt faults, or is it thin-skinned without sub-salt dynamics?
- Is ice-load induced faulting limited to salt floored basins?

Since ice-load induced faulting is yet just poorly studied, we do not know whether this process is limited to salt-floored basins. Testing needs both seismic profiling in the salt floored NEGB and the Pomeranian Bay NE of the salt pinch-out. Other questions are:

- Which of the Quaternary tunnel valleys are related to deep rooted faults?
- How important is the angle between advancing ice-sheet front and the strike of inherited faults?
- What is the effect of ice-load on inverted and strike-slip faults?
- Is there an increase or decrease of ice-load induced faulting towards the maximum extent lines of the glaciations?

#### 3.2.2 Salt tectonics and fluids

According to the traditional view salt diapirism in the NEGB (and other Paleozoic and Mesozoic salt basins world-wide) started above extensional basement faults as along the Glückstadt Graben or the consequence of thin-skinned extension and reactive, active and passive diapirism. However, there is no obvious reason not to assume that salt deformation started during salt precipitation,

similar to the Levant Basin. The gravity gliding initiated shortening and salt pillow growth even without significant sediment coverage. Later on the rim-synclines were filled by sediments and the differential load caused passive diapirism (downbuilding). After burial salt tectonics continued; first due to lateral varying sediment load and later during inversion. The confirmation of this hypothesis would cause a paradigm shift. The conceptual model would be much simplified: Basic principles like basin subsidence, basin floor tilt and resulting lateral salt flow would account for shortening in the central basin and – consequently – for the initiation of diapirism. Sub-salt faulting or head-room generation by thin-skinned extension that is an integrated part of the reactive-active diapirism concept would no longer be needed. Basic questions are:

- Are salt pillow always located above deeper faults?
- Is it possible to image intra-salinar Zechstein units?
- Is there evidence for fluid escape from the Zechstein as observed from the Messinian salt giant in the eastern Mediterranean?

### 3.2.3 Other upcoming objectives

Beside the overarching questions about ice-load induced and salt tectonics other scientific objectives will be addressed.

- What is the extent of the West Holstein, East Holstein, East Holstein-Mecklenburg Blocks, and how are these structures related to the Glückstadt Graben and Ringkøbing-Fyn High?
- What is the timing and origin of the Grimmen High?
- What is the timing and origin of the NW-SE striking faults within the Cretaceous and Jurassic strata in the western-most Pomeranian Bay?
- How does the fault system in the western Pomeranian Bay affect the island of Rügen?
- The elongated Upper Cretaceous antiforms along the southern STZ – do they represent inversion structures or contourites?

Within the Bay of Kiel, several troughs and boundary faults have been proposed by various authors. Their relation to the Glückstadt Graben and the NW-SE trending faults between the Ringkøbing-Fyn horst structures is unknown. The Grimmen High is a peculiar feature that has been interpreted as a drag-related salt anticline or strike-slip feature (see chapter 2). Its origin can be considered as highly uncertain. There are several options to explain faults in Cretaceous and Jurassic strata in the very western Pomeranian Bay between 12° and 13° E and 54°40'N and 55°10'N. The southward limit of the faults may either represent the southern margin of a fault swarm related to the STZ, or the limit marks the NE pinch-out line of the mobile Zechstein. North of it no mobile stratum decouples sub-salt faults from Post-Permian strata. Understanding of the fault system may help to decipher the structural overprint of the island of Rügen.

Finally, we intend to address the question whether the thickening of the elongated Upper Cretaceous strata along the southern rim of the STZ results from current moderated sedimentation or inversion.

### 3.3 Survey Layout

(C. Hübscher, V. Damm, C. Juhlin, C. Krawczyk, M. Malinowski, V. Noack, E. Seidel)

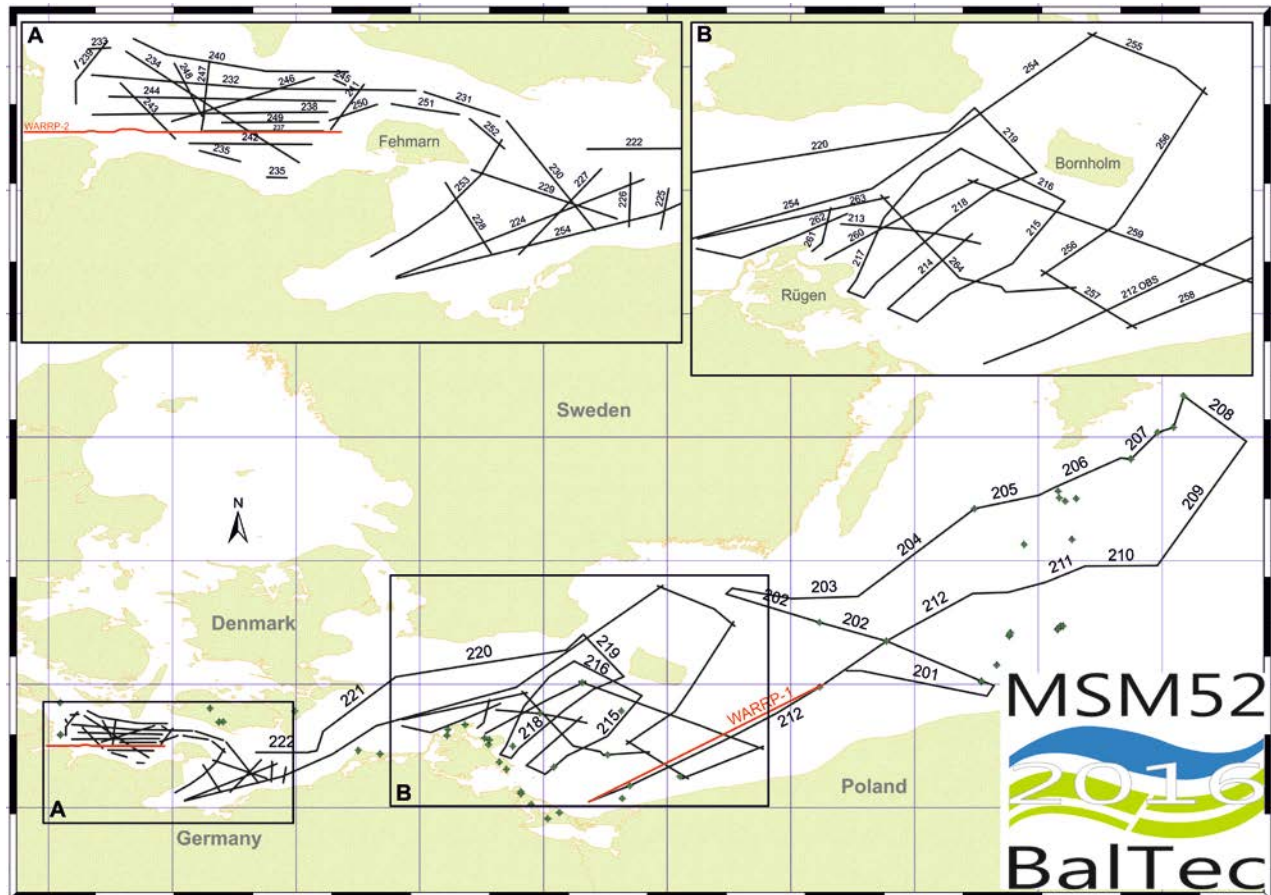


**Fig. 3.3.1** Reflection seismic profiles of MSM52.

The MSM52 seismic lines (Fig. 3.3.1) were mainly designed in accordance to the initial cruise proposal. However, several additional and previously unforeseen factors had to be considered. The BGR replaced the lead-in cable of their seismic streamer in a way that the underground could be imaged gaplessly up to the seafloor. This was the consequence of the decreased reflection angle from the seafloor to the proximal hydrophone groups. Consequently, there was no need to measure each profile twice as proposed in the initial cruise proposal. The gained time was used to extend the working area and to map the geological features of interest in greater detail. The final survey layout of the cruise was subject to ferry trails, natural habitats, protection areas and the coastline below 10 meter water depth, a limit given to the length of the streamer. Underway findings and unplanned harbor calls for exchange of ship technicians further influenced the schedule and survey layout.

**Bay of Kiel:** The almost west-east trending profiles elucidate the relationship between the elongated anticlines as described by Al-Hseinat and Hübscher (2014) and proposed sub-salt faults. These profiles further show the northward extend of the Eastholstein and Eastholstein-Mecklenburg Troughs and will allow relating the link of the boundary faults with the NW-SE

trending faults between the Ringkøbing-Fyn High. The eastern ones of these faults are crossed by the eastward extension of the northern profile into the Bay of Mecklenburg. North-south striking profiles allow the stratigraphic correlation between the E-W profiles. These lines are also perpendicular to the Alpine orogeny and may show inversion structures, if present. The wide-angle reflection refraction seismic profile was designed to image the crust from the eastern Glückstadt Graben to the presumed northward prolongation of the Eastholstein-Mecklenburg Trough.

**Mecklenburg Bay:** Similar to the scientific aims in the Bay of Kiel, the profiles have been designed to unravel the impact of sub-salt faulting on salt tectonics, crestal graben evolution and glacial erosion. In opposite to the Bay of Kiel, subsalt tectonics is less pronounced.

**Mecklenburg Bay to Hanø Bay transect:** These long NE-SW striking profiles run across the Grimmen High, the pinch-out line of the Zechstein northeast of the Grimmen High, the West Pomeranian fault system and finally the Sorgenfrei-Tornquist Zone itself. Data will therefore elucidate the major structural elements of the Baltica-Avalonia Suture zone and the Zechstein geometry from the Northeast German Basin to the basin margin, which is needed to understand initial salt creep towards the subsiding central Northeast German Basin.

**Pomeranian Bay between Rügen, Bornholm and Polish Coast:** The majority of these profiles will help studying the West Pomeranian fault system, the Teisseyre-Tornquist Zone including the Rønne Graben and the structural evolution of Rügen. These lines further imaged the postulated Cretaceous contourite southeast of it. No Zechstein salt is present. The wide-angle reflection refraction seismic profile here (chapter 5.2) was designed to image the deeper crust of the Teisseyre-Tornquist Zone.

**Profiles north-east of Bornholm:** An analysis of vintage seismic data by the working group of Chris Juhlin at Uppsala University (Sweden) suggested the presence of shallow subsurface faults on the Baltic Shield in the territorial waters of Sweden. Ice-load induced tectonics had been discussed as a possible trigger. The working area was consequently extended to the north in order to image these fault systems.

### 3.4 Relevance of the Seismic Survey to BGR's Project "TUNB"

(V. Noack, V. Damm)

BGR's strong interest to acquire new seismic data in the Baltic Sea is linked to the goals of the project "Subsurface Potentials for Storage and Economic Use in the North German Basin (TUNB)". The TUNB project originated from a growing interest in the deep subsurface in response to discussions on new technologies such as carbon dioxide capture and storage, storage of renewable energy, and exploitation of geothermal energy. In 2014, the state geological survey organisations (GSO) of the north German federal states and BGR (partner and coordinator) started the construction of a comprehensive and harmonised 3D model of the North German Basin (NGB). The model will comprise 13 main stratigraphic horizons, based on lithostratigraphic horizons from the "Tectonic Atlas of Northwest Germany and the German North Sea Sector" (GTA) in the west and seismic reflector horizons from the "Geophysical Atlas of the German Democratic Republic" in the east (Baldschuhn et al. 2001, Reinhardt 1991), including structural features such as salt structures and faults.

The German sector of the Baltic Sea is characterised by a lack of comprehensive geological data sets and seismic interpretations to extend the 3D model from onshore across the coastline into the Baltic Sea. The last seismic acquisition survey of BGR in the Baltic Sea (PQ-96) was conducted in 1996. Its aim was to analyse the basin evolution, and to detect the deeper crustal structure and the position of the Moho by means of long seismic transects (DEKORP-BASIN RESEARCH GROUP 1998). Information on Paleozoic to Cenozoic structures were analysed and presented in seismic travel time maps within the BGR research project SASO I (Schlüter et al. 1997). The authors revisited data obtained by the former consortium PETROBALTIC. The latter obtained a dense seismic profile grid of 1 x 2 km spacing for the offshore area between Darß Peninsula and the southwestern shelf region of Rügen Island and drilled four offshore wells in order to investigate the hydrocarbon prospectivity of the deep lying Paleozoic sediments in the 1980's (Rempel 1992). A recent reinterpretation of these seismic profiles has been carried out by CEP (Central European Petroleum) who reprocessed and digitised a number of profiles. Since 2012 most of these data are used for structural interpretations within the framework of the project USO (Underground Structural Model of the Southern Baltic Sea), a joint research project of the State Agency for the Environment, Nature Conservation and Geology of Mecklenburg-Western Pomerania (LUNG) and the University of Greifswald (Obst et al. 2015).

Baltic Sea data acquired in the past by research institutes and the E&P industry show high variability in data quality and target resolution. Navigation data of older seismic lines are of limited accuracy. Depth resolution is adjusted and focused on the specific target horizons and only selected regions are covered with dense line grids. The new data of the MSM52 cruise bridge still existing gaps between seismic data sets and previous interpretations. They are of significant importance for extending the 3D model of the North German Basin into the German Baltic Sea Sector.

### **3.5 Marine Mammal Observation to Comply With Environmental Best Practice Standards**

(Volkmar Damm, Gareth Allen)

#### **3.5.1 General Remarks**

BGR applies own best practice measures to comply with environmental standards of sustainable marine research and for impact mitigation while operating seismic sources even in case no precaution measures are requested with the research permission of the coastal states.

This commitment is identical with the worldwide well accepted JNCC rules (JNCC, 2010) for seismic operations negotiated by the British Joint Nature Conservation Committee.

The research program of the cruise MSM52 involved seismic operations in German, Danish, Swedish and Polish waters. Special preconditions for impact mitigations during seismic surveying were given by the Danish and Polish authorities.

The Swedish and German Governments did not require that marine mammal observers (MMOs) are carried aboard seismic survey vessels. However, in the adoption of best practice to international standards, BGR implemented a MMO regime aboard the RV Maria S. Merian Explora for all activities involving the use of a noise source array.

The Guidelines set down in August 2010 by the UK's Joint Nature Conservation Committee (JNCC, at [www.jncc.gov.uk/marine](http://www.jncc.gov.uk/marine)) were adopted for this survey. The purpose of the JNCC

Guidelines is to minimise the risk of possible injury from seismic survey source operation to marine mammals including seals, whales, polar bears and walrus.

There was one certified MMO of MSeis PAM SYSTEMS/UK contracted to fulfil the obligations for impact mitigations in Polish and Danish waters and to follow BGR's best practice standards for seismic operations during the full survey of cruise MSM 52.

The MMO was assisted by one member of the BGR team who had previously completed a training course, recognised by JNCC, in marine mammal observation techniques and procedures.

Two PAM systems were employed on the vessel during the cruise, primarily for marine mammal mitigation but additionally for comparison purposes:

1. **MSeis Night Hawk III** PAM system comprising of a 4-element towed array and acoustic processing system

([http://www.mseis.com/media/assets/MSeis\\_Night\\_Hawk\\_III.pdf](http://www.mseis.com/media/assets/MSeis_Night_Hawk_III.pdf)) using the PAMGuard analysis software (<http://www.pamguard.org/>), setup and operated by the PAM operator, and

2. **Sercel's QuietSea™ system** (<http://www.sercel.com/products/Pages/QuietSea.aspx>) which processes and analyses sound from both the seismic streamers and additional hydrophones on the gun arrays. QuietSea™ system is a new Sercel product which was recently purchased by BGR. It is fully integrated in the Sercel seismic acquisition units and operates automatically. During the first week a field service engineer of Sercel was onboard for customer support.

The contracted MMO/PAM operator was responsible for filling in all JNCC forms relating to seismic operations, visual and acoustic effort, sightings and acoustic detections with the MSeis PAM. Furthermore the MMO/PAM operator was responsible for providing advice on the application of the JNCC Guidelines.

The roles of the MMOs were as follows:

Conduct 30 minute (for waters less 200m deep) pre-shooting watches of a 500m exclusion zone around the source array to ensure the absence of marine mammals before the commencement of soft-starts.

To monitor soft-starts of the seismic array to ensure a minimum of 20 minutes (and no greater than 40 minutes) in duration.

To ensure that marine mammals have the opportunity to leave the survey area and request a delay to the soft-start if a marine mammal is sighted within the exclusion zone.

To advise the crew on the procedures set out in the JNCC Guidelines and to provide advice to ensure that the survey programme is undertaken in accordance with those Guidelines.

To organise watches in daylight hours, and so document any marine mammal sightings. To operate the MSeis PAM system and to ensure the absence of marine mammals before the commencement of soft-starts during periods of poor visibility e.g. during fog and darkness.

To document and report all source array use hours, observation effort hours, mammal sightings and mitigation and compliance issues.

The JNCC Guidelines state that MMO/PAM operators prioritize watches so that they are available for pre-shooting searches but that additional visual or acoustic watches can be performed if time allows acquiring information on the presence of marine mammal species.



Characteristic	Value	Unit
Number of airgun sub-arrays	2	
Number of airguns in each sub-array	4	
Inter-sub-array distance	18.6	m
Airgun type either GI-guns or G-guns	GI-gun / G-gun	
Airgun volume	150 / 250	inch <sup>3</sup>
“ “	2.46 / 4.1	l
Total number of airguns	8 / 8	
Total array volume	1200 / 2000	inch <sup>3</sup>
Total array volume	19.7 / 32.8	l
Source depth	3 / 6	m
Shot interval	9 and 10 / 30 / 60	sec
Nominal working pressure	2400	psi
Nominal working pressure	165	bar
Peak frequency	78 / 37	Hz
Bandwidth (-3dB)	143.3 / 64.3	Hz
SEL (zero to peak)	247 / 248	dB re 1 $\mu$ Pa @ 1m

**Tab. 3.5.1.1** Summary of seismic source characteristics relating to mitigation.

#### *Air-gun array and soft-start procedure*

A summary of seismic source characteristics, as required by JNCC, relevant to mitigation used on the RV Maria S. Merian during the 2D seismic survey are given in Tab. 3.5.1.1. Both sub-arrays were fired simultaneously.

The soft-start procedure used involved ramping up the acoustic power by increasing the number of guns while maintaining the operational pressure. Guns were fired at 18 s intervals starting with a single gun and adding in a new gun every 4 minutes until all 8 guns (totaling 1,200 and 2,000 in<sup>3</sup>, resp.) were fired 24 minutes after the start of the soft-start - in line with the JNCC Guidelines.

### **3.5.2 Conventional Visual Observations**

Visual observations for marine mammals were carried out during daylight hours primarily during seismic source pre-shooting search periods, but also at other times (before pre-shooting search, from soft-start to start-of-line and all daylight operations). The MMO (i.e. trained member of science party) was equipped with a binocular and positioned at the bridge. He was assisted by crew members and other members of the science party to guarantee continuous observations. All observation activities are documented in the dedicated watch protocols. No visual sightings of marine mammals were done during the seismic survey operations. But two bottlenose dolphins were spotted when entering Kiel harbor March 28<sup>th</sup> (see Fig. 3.5.2.1). These animals were observed in the area since February 2016 over 6 weeks.



**Fig. 3.5.2.1** Sightings of two bottlenose dolphins in Kiel harbor.

### 3.5.3 Conventional Passive Acoustic Monitoring PAM

Passive acoustic monitoring was used to detect marine mammals in the vicinity of the seismic source during pre-shooting search periods if these were in periods of poor visibility e.g. darkness, fog, etc. During dedicated acoustic monitoring periods the PAM operator would listen to filtered (i.e. to remove noise such as seismic shots) medium-frequency sounds through noise cancelling headphones and observe graphical displays of low- and high-frequency tonal and impulsive sounds on the PAMGuard displays. Additionally, automatic acoustic monitoring was carried out during all periods, when visual observations were prioritised.

The hydrophone array and sound processing and analysis system used was a Night Hawk III PAM System supplied by MSeis PAM SYSTEMS (<http://www.mseis.com>). The system comprised of a four-element array and a depth sensor at the end of a 200 m tow cable which carried power and analogue signals. The array (except deck connector) was rated to a depth of 10 m.

*Specifications of Night Hawk III PAM System designed by MSeis PAM SYSTEMS:*

Hydrophone:	Custom built -201 dBV re 1 microPa effective sensitivity. Near-flat response 0 to 180kHz, omni-directional (tested at 50, 75 and 100kHz)
Cable:	Custom length deck cable. In water cable to 300m.
Preamplifier:	PA2 (MSeis in house design and build)
Channels:	4
Depth Sensor:	Pressure sensor 4-20 mA
Bandwidth:	4Hz - 180kHz +/-3dB
Acquisition:	NI DAQ card; sampling to 500KS/s, external USB sound card; sampling to 192KS/s
Software & Data Logging:	Pamguard

With the conventional MSeis PAM system there was no acoustic detection during the full period of the cruise. The PAM system was setup for triggered recordings with database logging for post survey analysis as effort was prioritised on visual watch except for the aspects of the survey conducted in Polish waters in accordance with the licence agreement. Whilst in Polish waters the MMO switched to night time monitoring (recordings triggered by operator); and the visual watch carried out by members of the scientific crew.

Since all PAM data including the data which was acquired during unattended operation was stored the absence of localisations can be verified by subsequent analysing which must be subject to further post-processing and interpretation.

### 3.5.4 QuietSea System for Passive Acoustic Monitoring

QuietSea™ is a recently developed Marine Mammal Monitoring System designed by Sercel to detect the presence of marine mammals during seismic operations without towing additional PAM equipment behind the vessel. This streamer integrated system is operated as a peripheral device to Sercel's seismic data acquisition unit SEAL 428.

QuietSea™ system uses two classes of data to cover a broadband frequency spectrum:

- the seismic data (using the SEAL interface) to detect vocalizations in the (low-frequency) seismic bandwidth from 10Hz to 200Hz with usual seismic sampling frequency of 2ms and
- (high-frequency) data, provided by additional QS streamer modules integrated within the Sercel seismic streamer (Sentinel, Sentinel RD and Sentinel MS) and other QS auxiliary modules to detect vocalizations in the bandwidth of 200Hz to 96kHz.

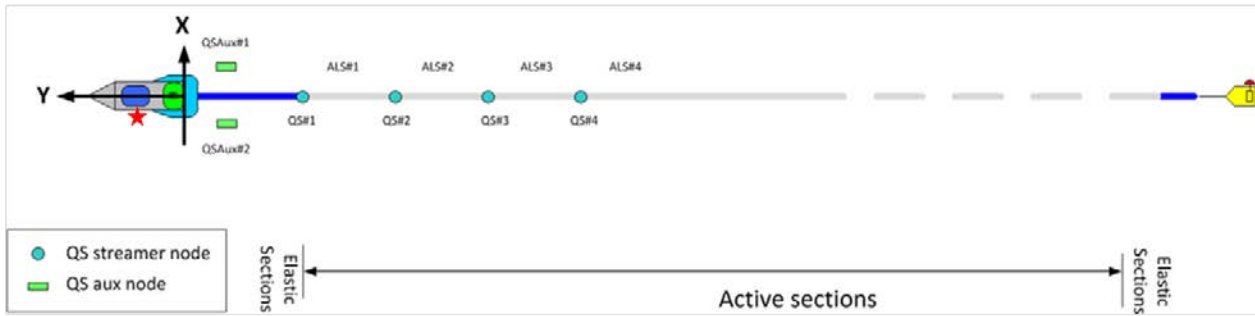
This potentially allows for enhanced marine mammal detection capabilities in a wide frequency listening range that covers a large variety of vocalizing cetacean species Monitoring is conducted by automated detection and localization algorithms.

During the 2D seismic operation of PANORAMA-2 for the high-frequency detections 4 QS streamer modules (Fig. 3.5.4.1, left) plus 2 QS aux modules (Fig.3.5.4.1, right) were employed.



**Fig. 3.5.4.1** QS streamer module (left) and QS auxiliary module (right) within protective cage, frequency bandwidth 200Hz to 96kHz

The QS streamer modules were integrated between the first 4 active sections of the streamer, separated 150 m to each other, the QS aux modules were connected to the gun floats (Fig. 3.5.4.2).



Position of the QS aux node at the guns (GSAux#1, GSAux#2):

distance between both guns 14 m =>  $X_1=7, X_2=-7$

distance to stern 25 m =>  $Y=-25$

depth is 6 m =>  $Z=6$

center of gun arrays:  $X=0; Y=-25; Z=6$

Position of the QS aux node at the vessel (red asterix):

distance to y-axis 7.7 m =>  $X=7.7$

distance to stern 30 m =>  $Y=30$

depth is 5 m =>  $Z=5$

**Fig. 3.5.4.2** 2D seismic vessel configuration of QS high frequency components.

During the cruise MSM52 for low-frequency detection 53 channels of the streamer hydrophone groups were selected separated 50 m to each other with a nearest offset of 58 m to the vessel and a farthest offset of 2710 m. The detailed position of each QS node with reference to the vessel was configured in an appropriate node file to be read in into the QS software. QuietSea software allows monitoring acoustic events in the high- and low-frequency range separately. The several sources of anthropogenic impulsive sounds of the vessel (produced by the airguns and echosounders), can be filtered out. All acoustic events are logged in a protocol and stored in a QuietSea database. The QuietSea system claims to localize a marine mammal when a vocalization is detected by several sensors. Detections at individual sensors which do not meet the condition to be verified by at least three sensors are not considered for localization. During the full survey period a number of events were detected, but no record could be verified as the vocalization of marine mammals. The database is currently subject to post-processing and will be still re-analyzed.

### 3.5.5 Conclusions Regarding Mitigation & Compliance with JNCC Guidelines

The JNCC (2010) ‘Guidelines for minimising the risk of injury and disturbance to marine mammals from seismic surveys’ were followed throughout the survey. Three independent methods (visual and 2 PAM systems) were used for mitigation measures. There were no occasions when mitigating action was required. The survey was compliant with the JNCC guidelines.

## 4 Narrative of the Cruise

(C. Hübscher)

The RV MARIA S. MERIAN berthed in Rostock harbor in the morning of February 27<sup>th</sup>. Unloading of the containers from the previous cruise started immediately, followed by the mobilization of the scientific gear of the University of Hamburg, the BGR (Hanover) and the Polish Academy of Science (Warsaw). The volume of the loaded gear corresponded to that of 8 containers. The marine gravimeter started to measure which continued until the end of the cruise. Deck and lab installations lasted until the late evening of February 29. A ship's tour was held for Dr. Hoth from the Federal Ministry for Economic Affairs and Energy and other visitors. RV MARIA S. MERIAN disembarked in the morning of March 1<sup>st</sup>, followed by some engine tests in the north-eastern Bay of Mecklenburg. We called Warnemünde harbor around noon and some technicians left the vessel. The transit to the western Pomeranian Bay started shortly afterwards. Early the next day the BGR group began to deploy their about 2700 m long seismic cable. The buoyancy was tested by various speeds and some additional floatation tubes were attached to the cable. The visual search for marine mammals started in the early afternoon, but no one could be detected. In the late evening two arrays of seismic signal sources were deployed and tuned. Based on some test measurements the final recording parameters were determined and we switched to production mode. Since the late evening of March 2<sup>nd</sup> we continuously collected multi-channel seismic, Parasound, Multibeam and Gravity data on a 24/7 schedule.

The first profile crossed two production wells in Polish waters, continued to the Yoldia well and ended within Hanø Bay (Sweden). Since March 3<sup>rd</sup> 05:00 the towed gear was watched over by guard vessel NORDSØN in order to prevent that any vessel crosses the towed seismic cable. Profiling continued on north-easterly courses along the east coast of Øland towards east of Gotland where we arrived on March 5<sup>th</sup>. After a short NW-SE striking profile across a suggested glacial sedimentary feature called drumlin we changed course again and profiled south-westwards along the border between Swedish and Latvia's and Lithuania's waters, respectively. Seismic profiling ended north of Swinoujście on March 7<sup>th</sup> in the afternoon. The fast transit to Warnemünde harbor ended on the 8<sup>th</sup> in the morning where two technicians disembarked. During the night to the 9<sup>th</sup> we sailed back around Rügen into Polish territorial waters where we started deploying 15 ocean-bottom seismometers along a 120 nm long profile crossing the Tesseyre-Tornquist Zone. 8 clustered G-Guns were used as the seismic source which released their signals during 30 hours. On the 11<sup>th</sup> we recovered the OBS which lasted until the 12<sup>th</sup> in the early morning. Afterwards we called Sassnitz harbor where technical and scientific crew members were exchanged. In the afternoon we commenced reflection seismic profiling between Rügen and Bornholm and investigated the Caledonian Deformation Front and the West-Pomeranian Fault System until March 14<sup>th</sup>. In the night to the 15<sup>th</sup> we investigated the transition from Baltica to Avalonia in the Kadettrinne. Salt pillows in Mecklenburg Bay were the scientific target of seismic profiles on the following day. We crossed Fehmarn Belt during the night to March 17<sup>th</sup> without any problems and continued profiling in the Bay of Kiel, which lasted until Saturday (March 19<sup>th</sup>) early morning. Afterwards we deployed 10 OBS between Fehmarn and the eastern Eckernförde Bay. Seismic signals were released during the night to Sunday. Colleagues from the University of Kiel had installed land station both on Fehmarn and along the southern coast of Eckernförde Bay, so the signals were recorded not only by the OBS. The recovery lasted until Sunday late evening.

During the night we collected gravity data where we could not measure with the streamer deployed. On Monday morning (March 21<sup>st</sup>) we called Kiel harbor for another crew exchange. In the afternoon the same day the reflection seismic gear was deployed again. Reflection seismic profiling in the Bays of Kiel and Mecklenburg was completed on March 22<sup>nd</sup>. One of the key profiles started in the south-western end of Mecklenburg Bay which is part of the North German Basin. The north-east directed profile crossed Grimmen High and the West Pomeranian Fault System between Darss and Falster and the Sorgenfrei-Tesseyre Zone between Bornholm (Denmark) and Skåne (Sweden). This about 350 km long seismic line ended in Hanø Bay (Sweden) on March 23<sup>rd</sup>. We collected two more seismic lines across the Tesseyre-Tornquist Zone and one more across the Rønne Graben until March 25<sup>th</sup>. We spent the last two days north of Rügen and collected seismic data which will be used to link regional data grids which have been collected during previous surveys. All scientific measurements stopped on Sunday March 27<sup>th</sup> in the morning. When the seismic equipment was on deck we started our transit back to Kiel where we arrived on Monday 28<sup>th</sup> in the morning. We disassembled all our installations and packed all gear in boxes and containers. Ship was unloaded on the 29<sup>th</sup> and the BalTec cruise MSM52 was over.

## 5 Preliminary Results

### 5.1. Processing of Multi-Channel Seismic Reflection Data

(M. Schnabel, M. Engel)

Seismic data processing was performed using a Linux workstation with ProMAX™ 2D, Version 5000.0.1 licenses. The workstation has two Quadcore AMD CPUs, a RAM of 32 GB and a 170 GB system hard drive. The operating system is CentOS Linux 5.0. Data were stored on two internal hard drives and a backup was carried out to an attached NAS system.

Onboard processing was done for lines BGR16-212 to BGR16-264 including the following steps: geometry setup, data and geometry input, prestack processing to enhance signal quality, velocity analysis, multiple elimination, data stacking, Kirchhoff migration and post-processing.

#### 5.1.1 Geometry Setup

The same streamer and airgun setup was used during the entire MSM52 cruise as sketched in Fig. 5.1.1.1. The geometry of the source and the receivers was set up in relation to the vessels MRU antenna position according to the precise measures of the Parker report. The active streamer length was set to 2700 m with 216 channels for all seismic lines. In ProMAX the 2D Marine Geometry Spreadsheet was used. It includes the following steps which have to be carried out in the geometry setup sequence:

*File. UKOAA Import:* The navigation data from the ship was transformed into rectangular UTM (zone 33N) coordinates and reformatted in the format “STANDARD UKOAA 90 Marine 2D”. The shot numbering from the Master PC was written to the field “Station”.

*Setup:* All lines were acquired with 12.5 m nominal receiver spacing and 25 m nominal source station interval. The other parameters changed and are reported in the acquisition logs. All units are given in meters.

*Sources:* The streamer azimuth has to be calculated using “auto azimuth”. The algorithm used for this by ProMAX is very crude. It is based only on the first and last source point, the calculated

azimuth is assigned to all source positions. Therefore turns before and after straight profile lines have to be removed (shooting continued during turns between profile lines). The column “Src Pattern” has to be filled with the number of the pattern defined in the next step (here number 1). Shotpoint interval and error were checked by the QC tool. The navigation files sometimes show wrong coordinates due to GPS malfunction – these positions are interpolated in the table and also in the navigation file.

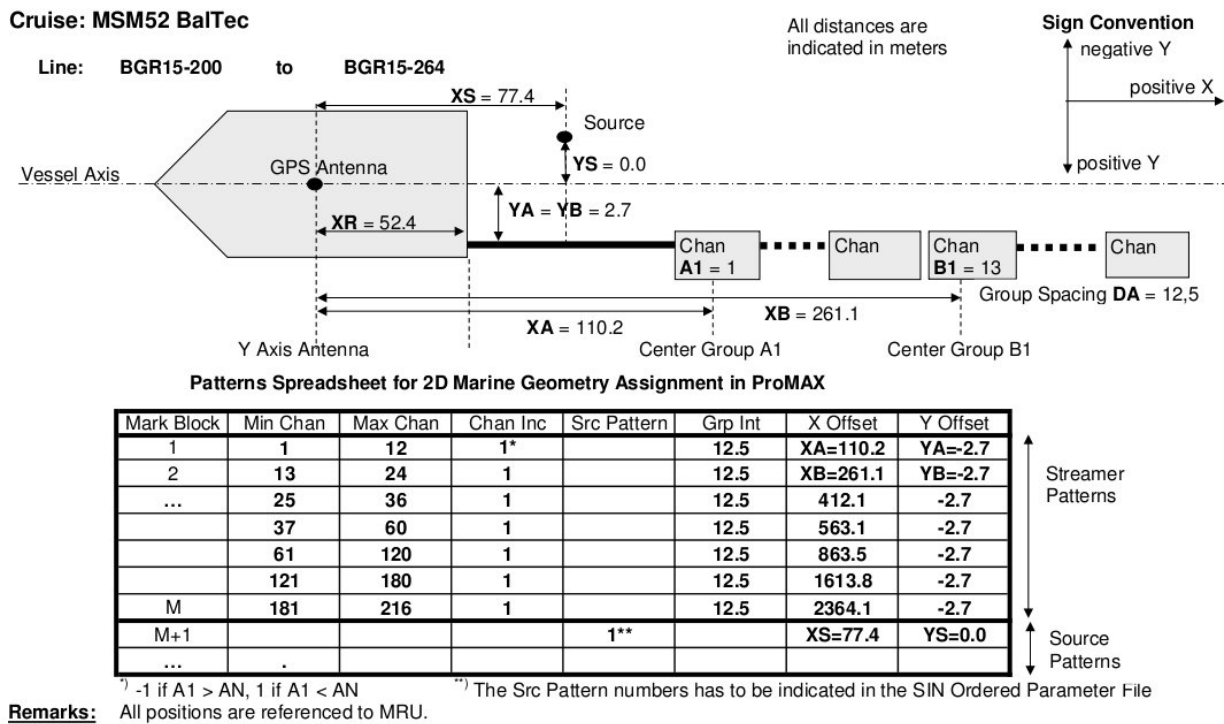


Fig. 5.1.1.1 Sketch of the streamer and airgun geometry aboard of RV S.M. Merian.

**Patterns:** The streamer and source patterns have to be defined according to the spread-sheet in Fig. 5.1.1.1.

**Bin:** The binning consists of three steps:

1. Assign Midpoint.

2. Binning. Source station tie to CDP number: During this cruise, the seismic recording continued during the turns. The first shot (start point of the straight profile line after a turn) was noted in the acquisition logs and this shot should be entered as station tie to CDP number;

CDP Number tie to source station: 10000. This tie fulfils BGRs standard for CDP numbering: The first station with full coverage is tied approximately to CDP 10000. Distance between CDPs: 6.25 m. This implies a nominal CDP coverage of 54 (for 216 channels) in case of a shot increment of 25 m. Binning was done for CDP locations and receivers (CDP numbers and receiver numbers increase with increasing shot number).

3. Finalize Database.

*TraceQC*: Quality control of binning. Here two checks are undertaken:

- Checking the computed offsets with the offsets given in the streamer plan by comparing the values for the last hydrophone group (channel 216) and nearest hydrophone group (channel 1).
- Checking if the source and receiver locations (in UTM coordinates) are behind the vessel in relation to the sense of direction.

A further quality control was done by using the graphical display tools of the database application:

- CDP fold map (Database => View => Predefined => CDP fold map). X\_COORD and Y\_COORD – Axes; FOLD: Colour coded and as histogram.
- CDP fold table (Database => View => Tabular => CDP): List of CDP Number, FOLD, X\_COORD and Y\_COORD.

*SEG-D input from NAS and geometry application*: Data were copied from the NAS hard drive to the internal hard drive of the processing workstations. The SEG-D Input module fails, if the path name to the SEG-D files is too long. An acceptable work-around is to create a soft-link in the root directory to the SEG-D-file directory.

The shot-ordered data consists of 216 data channels at 1 ms with a recording length of 8500 ms. With the “Display ensemble information” set to YES a summary of all imported shots is written to the log-file. This is helpful in case that there are problems during acquisition. The shot counter from the Master PC was remapped from the SEG-D main header values using the option “Input/override main header entries: SH\_PC, BGR counter,5c,,1649/” within SEG-D input.

*Resampling (Resample/Desample)*: The seismic data has been acquired at 1 ms sampling rate. To speed up the onboard processing, the data has been re-sampled to 2 ms applying a high-fidelity anti-alias filter.

*SOD time correction (Header Statics)*: The Sercel acquisition system starts registration 120 ms before releasing the airguns. This time delay has been verified by the direct water wave arrival on the groups near to the source.

*Geometry Apply (Inline Geometry Header Load)*: With this ProMAX module, the geometry information from the database (created during geometry setup) were written into the trace headers. The match between navigation and seismic data was done with the time stamp, using the headers “TIME\_SHOT” and “DAY\_SHOT” with a time tolerance of 1 sec. Finally, the Trace Header Math module inserted an entry for the line number header word. The altered data was written to hard disk as new prestack data set (Disk Data Output).

*SEG-Y export*: To facilitate processing with other software packages, a SEG-Y version with merged navigation and a trace length of 5 sec was exported.

### 5.1.2 Pre-Processing

*Wavelet Analysis*: We used an unconventional GI-gun array which was not perfectly tuned. Due to the injector mode, the bubble was successfully removed. However, the source wavelet superposition of the GI-guns within each clusters and the superposition of both cluster remains unclear. Therefore, we carefully analysed the shape of the produced seismic signal. We stacked (ProMAX module “Ensemble Stack/Combine”) the direct wave recording from the first receiver group of approximately 100 shots along profile BGR16-202 over relatively deep water. A 200 ms wavelet was generated using the module “Wavelet Generation”. With “Filter Generation”, a



matching filter was designed which converts the data to minimum phase. Finally, “Filter Application” applies the filter to the whole data set. The result is shown in Fig. 5.1.2.1.



**Fig. 5.1.2.1** Extracted wavelet for cruise BalTec (left wiggle). Resulting wavelet after the application of the minimum phase filter (right wiggle).

*Bad Trace Editing:* The shot gathers were checked for bad traces. If present, these can be killed and thus been excluded from further processing. Anyway, the recorded data recorded were of very good quality with no bad traces, which had to be deleted.

*Bandpass Filter:* After the examination of the interactive spectral analysis a zero phase Ormsby bandpass filter of 8/15-250/450 Hz was applied to the data.

### 5.1.3 Velocity Analysis

*FK filter:* The dominating energy is due to multiple reflections within the water column between source and receivers. In shallow waters the angle of total reflection is already exceeded for hydrophones in the first ALS sections (33 m offset). In order to remove most of these arrivals as well as dominating refractions we rejected the strongest linear structures in the FK-domain. Afterwards subsurface reflections are much better visible before and after the remaining arrivals of the water waves. An example is shown in Fig. 5.1.3-1.

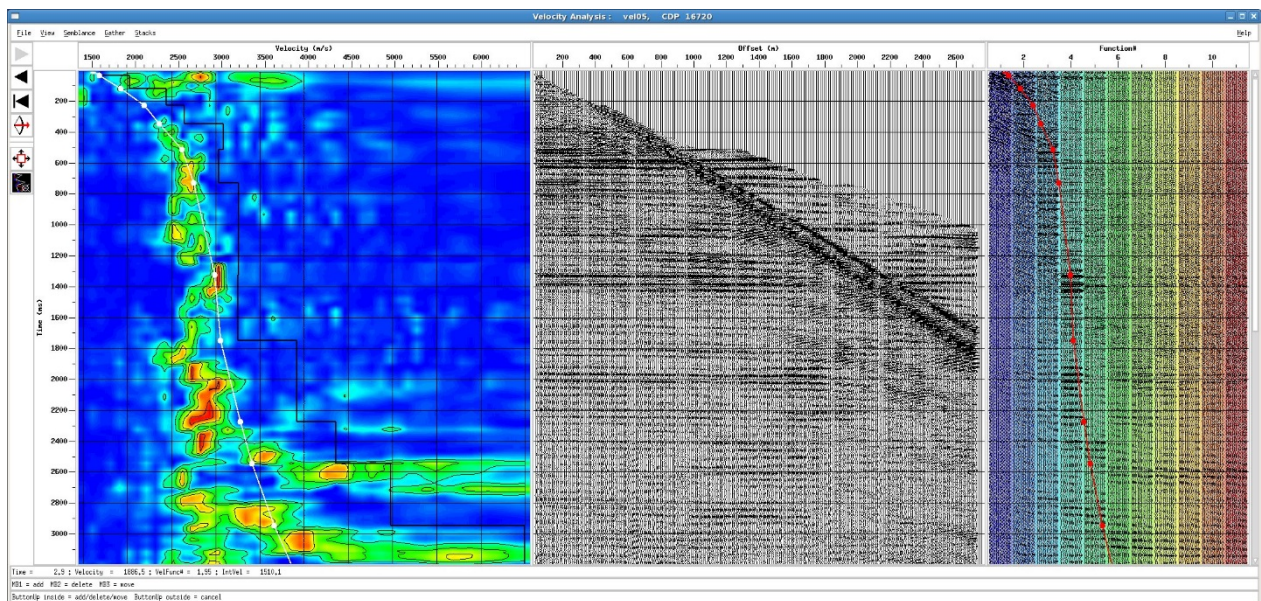


**Fig. 5.1.3.1** Example for the velocity analysis. The middle panel shows the NMO-corrected supergather – with primary energy arriving before the direct wave.

*Velocity Analysis:* First we perform a 2D supergather for a selected CDP increment combining 11 CDPs. The true amplitudes were recovered in a first iteration by a 1D velocity function from literature or refracted waves. During the velocity analysis precompute routine velocity functions are computed between minimum and maximum time guide values. During the velocity analysis velocities are picked for selected CDPs by comparing energy maxima in the semblance window, the hyperbolic fit to the reflectors in the gather window and enhanced amplitudes of the velocity functions. After the first iteration, a stacked gather can be computed in order to compare the lateral structure in the vicinity of the actual CDP where velocities are picked – extra CDPs can be incorporated in the supergather formation if reasonable. Furthermore, interval velocities are displayed online.

For the second iteration, the already picked velocities replace the 1D velocity function for the true amplitude recovery. Again, the precompute and analysis routine are executed and velocity picking can be improved. A third iteration serves as an extra check for QC. Afterwards, the velocity viewer allows smoothing the picked velocities as input for the migration later on.

#### **5.1.4 Multiple Elimination**

Due to the shallow water (10-60 m) multiple reflections are a major concern in the whole data set. For multiple suppression we briefly tested three methods from the ProMAX library:

- (1) FK filtering (rejecting multiple energy)
- (2) Radon filter (discriminating multiples in the tau-p domain)
- (3) SRME (using multiple periodicity and reflector horizons)

However, the approaches do work to some extent but mask also information which might be of interest at this early stage. Therefore, these schemes were not convincing for a general first robust onboard processing flow. Multiple elimination in the prestack domain needs more care and will be performed during the post-cruise processing.

#### **5.1.5 Stacking and Migration**

After careful analysis of the velocities, we corrected for spherical divergence (*True Amplitude Recovery*), normal moveout and performed a manual picked trace muting. We stacked the data up to the maximum offset of 2800 m.

After stacking, a predictive deconvolution removed successfully most of the strong ringing effects. The upper and lower gates for the deconvolution operator was picked from the stacked section focusing on a range of good signal to noise ratio. The success of the predictive deconvolution was tested by autocorrelation before and after predictive deconvolution. We applied poststack migration (*Kirchhoff Time Mig.*) using smoothed velocities.

#### **5.1.6 Post-Processing**

To reduce random noise, we applied a Wiener Levinson deconvolution in the F-X space (*F-X Decon*). To enhance the deeper signals with lower frequencies, we applied a time and space-variant filter (*Bandpass Filter*) which allowed frequencies between 16 to 60 Hz in the lower part of the section. A weighted mix over 5 traces was also applied (*Trace Mixing*). During export to SEG-Y, the shot number was mapped to byte position 197.

## 5.2 Wide-Angle Reflection Refraction Seismics

(M. Malinowski, J. Bülow, C. Hübscher)

During MSM52 cruise, two wide-angle reflection/refraction profiles (WARR) were acquired using Ocean Bottom Seismometers (OBS) from Institute of Geophysics University of Hamburg (10 units) and Institute of Geophysics, Polish Academy of Sciences (IG PAS) (5 units) (Fig. 5.2.1).

In each case, the anchors of the OBS were tied to the OBS with a rope (with a length of ca. 3 time water depth) in order to retrieve the anchors from the seafloor after recovery of the OBS themselves.

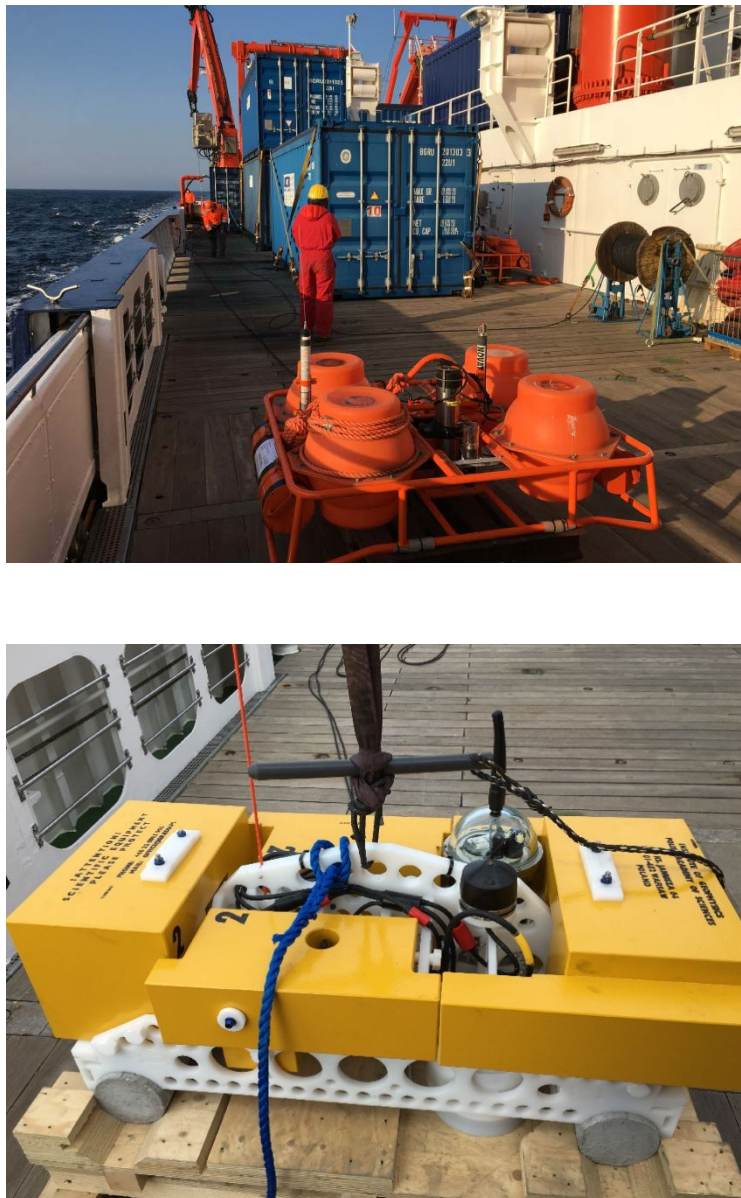


**Fig. 5.2.1** Top: Short period OBS unit from University of Hamburg. Bottom: Broad-band GURALP-OBS unit from IG PAS.

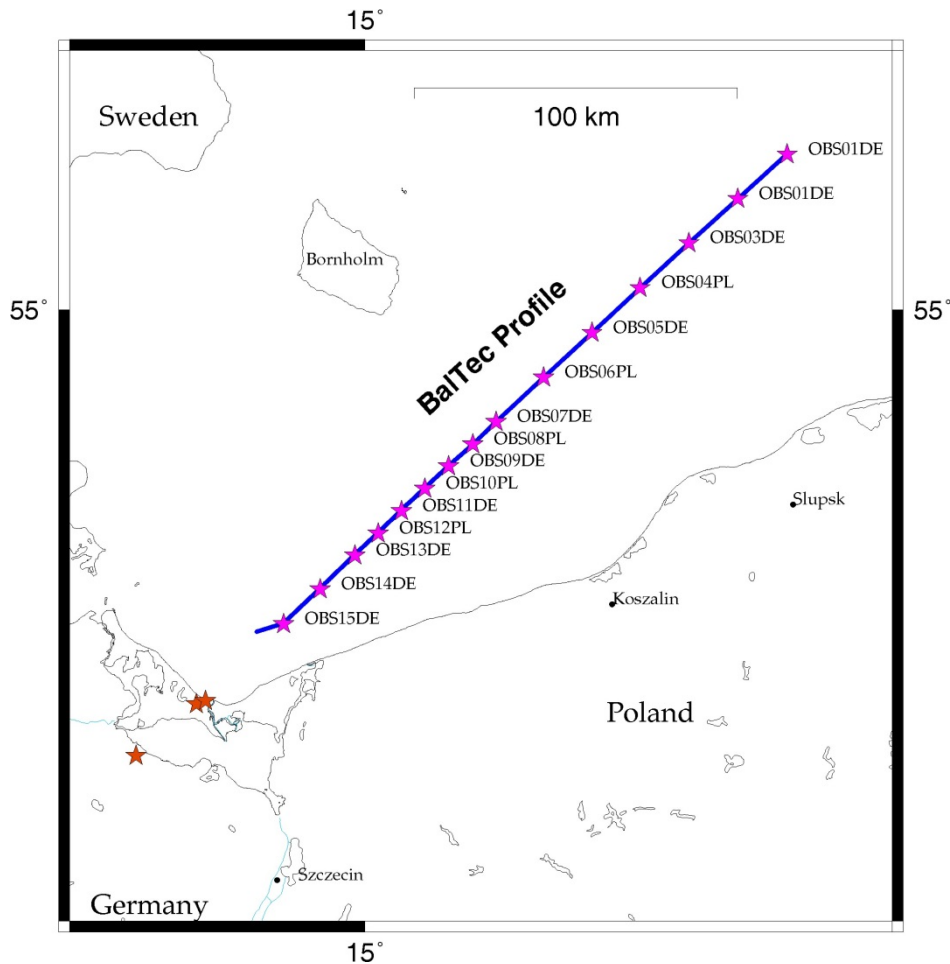


**Fig. 5.2.2** Location of the WARRP1 profile. Purple stars – OBS locations. Orange stars – location of the land stations. Blue dots – shot point locations.

The first WARR profile (WARRP1) was located in the Polish exclusive economic zone, running SW-NE across the Teisseyre-Tornquist Zone (TTZ), with a length of ca. 220 km (Fig. 5.2.2). It was coincident with the MCS profile BGR16-212. The motivation for shooting this profile was related to the fact that there are very contrasting interpretations of the crustal structure around TTZ, which are based on the data that are either not well documented or relatively sparse.

All available OBS nodes (15) were deployed along the WARRP1 profile. Because of the higher available sampling rate (2 ms vs 5 ms) for the Polish nodes, those units were placed closer to the TTZ locations. Also, to prevent data loss in case of the instrument failure, German and Polish nodes were located in turns. Location of the OBS units is shown in Table 5.2.1. Instruments were deployed on March, 9. The profile was shot in one-pass from SW towards NE on March, 10. Source array consisted of 8 G-guns with the total volume of 32 liters, operating at the pressure of 2000 PSI. Nominal shot interval was 60 s (ca. 120 m with a speed of 4 knots), however on the shallow water in the SW portion of the line, shots were fired with the reduced air gun array (4 or 6 guns only) and the shot interval was reduced to 30 or 45 s. Units were recovered on March, 11.

Initial data processing was performed onboard. Data were offloaded from the digitizers in the raw format and then 60-s long SEG-Y files were cut according to the GPS timestamps of the air-gun shots. Data comprised of 4 channels for each OBS unit: hydrophone and 3 vertical-component seismometer recordings with 3 different gains for the German units and hydrophone + vertical and two horizontal seismometer components for the Polish nodes. Subsequently, individual event-

oriented SEG-Y files were merged together for each channel to form common-receiver (OBS) gathers utilizing Seismic Unix scripts. Shot and receiver locations (in UTM coordinate system) were loaded into the .SU file headers and the offset was calculated using those coordinates. Finally, data were resampled at a common sample rate of 10 ms.

LONGITUDE	LATITUDE	DEPTH	STATION	UNIT
17° 00' 3.7800" E	55° 25' 18.3600" N	51	OBS01	German
16° 46' 5.4000" E	55° 18' 4.1400" N	71	OBS02	German
16° 32' 8.5200" E	55° 10' 52.0800" N	54	OBS03	German
16° 18' 18.0600" E	55° 03' 34.3200" N	67	OBS04	Polish
16° 04' 36.6000" E	54° 56' 14.4600" N	64	OBS05	German
15° 50' 50.4000" E	54° 48' 57.4800" N	67	OBS06	Polish
15° 37' 14.3400" E	54° 41' 36.3000" N	63	OBS07	German
15° 30' 39.3600" E	54° 37' 55.3200" N	63	OBS08	Polish
15° 23' 49.3800" E	54° 34' 17.1000" N	56	OBS09	German
15° 17' 1.4400" E	54° 30' 37.2000" N	63	OBS10	Polish
15° 10' 24.6600" E	54° 26' 56.0400" N	31	OBS11	German
15° 03' 43.0800" E	54° 23' 11.7000" N	23	OBS12	Polish
14° 57' 4.1400" E	54° 19' 31.0800" N	15	OBS13	German
14° 47' 10.6200" E	54° 13' 55.8600" N	15	OBS14	German
14° 36' 51.0000" E	54° 08' 9.3000" N	12	OBS15	German

**Table 5.2.1** Location of the OBS units along the WARRP1 profile.

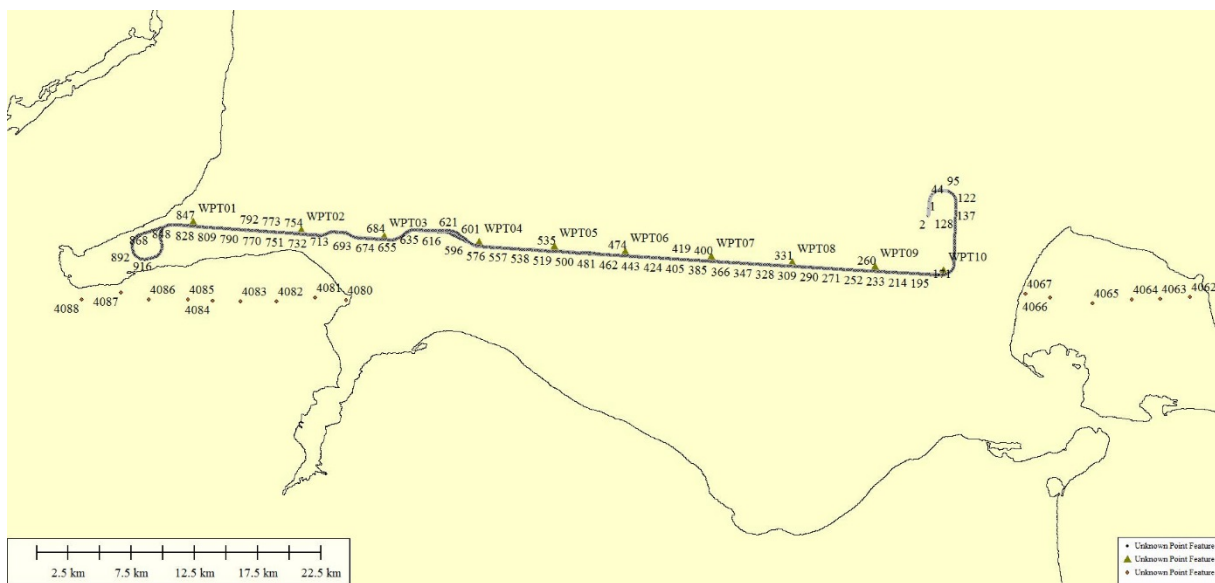


**Fig. 5.2.3** Location of the WARRP2 profile in the Bay of Kiel. Triangles mark the OBS positions. Shooting line is indicated by dots. Dots with numbers on land denote seismic land stations provided by the University of Kiel.

The second WARR profile (WARRP2) was located in the Bay of Kiel between Fehmarn and Eckernförder Bay. Due to the operational constraints, only 10 OBS units (only German ones) were deployed. As a complement to OBS acquisition, land stations were deployed by the University of Kiel (Fig. 5.2.3). The aim of this relatively short profile (65 km) was to create a structural model of the interaction between the Permo-Mesozoic sediments and their basement, including the salt velocity model.

LONGITUDE	LATITUDE	DEPTH	STATION
10° 55' 3.1200" E	54° 30' 0.4200" N	11	OBS10
10° 50' 4.1400" E	54° 29' 59.2200" N	14	OBS09
10° 44' 0.0000" E	54° 29' 58.8600" N	14	OBS08
10° 38' 1.0200" E	54° 29' 59.5800" N	17	OBS07
10° 31' 44.6400" E	54° 29' 59.4000" N	14	OBS06
10° 26' 30.4200" E	54° 30' 0.1200" N	15	OBS05
10° 21' 0.3600" E	54° 29' 59.5200" N	18	OBS04
10° 14' 1.1400" E	54° 29' 58.2000" N	12	OBS03
10° 07' 58.0200" E	54° 29' 58.9200" N	12	OBS02
10° 00' 1.6200" E	54° 30' 0.3000" N	25	OBS01

**Table 5.2.2** Location of the OBS units along the WARRP2 profile.

Location of the OBS units is shown in Table 5.2.2. Instruments were deployed on March, 19. The profile was shot in two-passes: from East to West and from West to East on March, 19-20th. This time, the source array consisted of 8 GI-guns with the total volume of 32 liters, operating at the pressure of 2000 PSI and fired in a GI mode. Nominal shot interval was 45 s, however some shots were fired with the reduced air gun array (4 or 6 guns only) and the shot interval was reduced to 15 or 30 s. Units were recovered on March, 20.

Data processing was similar to line WARRP1. Data from two shooting lines were merged together in the final SEG Y files.

### 5.3 Hydroacoustics

(N. Ahlrichs, L. Frahm, J.M. Stakemann, J. Stakemann, K. Knevels, I.L. Lydersen, E. Seidel, C. Hübscher)

In order to get detailed information about the seafloor morphology of the study area, the seafloor was surveyed by a SIMRAD EM122 echo sounder system. Generally, the system was acquiring data throughout the entire cruise. The system includes a hull-mounted transducer which periodically (12 kHz) emits a pulse and subsequently records the travel time after the signal was reflected at the seafloor. Knowing the sound velocity of the water column, the travel time of the signal thus provides information about the water depth.

The uppermost sediment layer was investigated by a hull-mounted PARASOUND DS III-P70 system (Atlas Hydrographic). By simultaneously emitting two primary frequencies between 19 and 23.5 kHz, a parametric frequency of around 4 kHz is created, allowing for a maximum penetration depth of approximately 200 m beneath the ocean floor. However, the penetration

capacity of the system strongly depends on the lithological properties of the sediment layer. Recorded data was digitized and subsequently stored in SEG-Y and PS3 format.

## 5.4 Gravimetry

(Heyde, I., Bülow, J.)

### 5.4.1 The Sea Gravimeter System KSS31M

During the cruise MSM52 the sea gravimeter system KSS31M of the Institute of Geophysics (University of Hamburg) was used. The KSS31M was installed in the gravimeter room one level below the main deck. The sea gravimeter was located approximately 1 m above the vessel's nominal water line, 0.88 m to portside from the centerline, and 53.20 m forward of the stern.

The gravimeter system KSS31M is a high-performance instrument for marine gravity measurements, manufactured by Bodenseewerk Geosystem GmbH. The KSS31M system consists of two main assemblies: the gyro-stabilized platform with the gravity sensor and a rack with the power supply, the system electronics and the data handling subsystem.

The gravity sensor GSS30 consists of a tube-shaped mass that is suspended on a metal spring and guided frictionless by 5 threads. It is non-astatized and particularly designed to be insensitive to horizontal accelerations. This is achieved by limiting the motion of the mass to the vertical direction. Thus it is a straight line gravity meter avoiding cross coupling effects of beam type gravity meters. The main part of the total gravity acceleration is compensated by the mechanical spring, but gravity changes are compensated and detected by an electromagnetic system. The displacement of the spring-mass assembly with respect to the outer casing of the instrument is measured using a capacitance transducer.

The leveling subsystem consists of a platform stabilized in two axes by a vertical, electrically erected gyro. The stabilization during course changes can be improved by providing the system with online navigation data. The control electronics and the power supply of the platform are located in the data handling subsystem unit. Online navigation data from the ship's system are sent with a rate of 1 Hz to support the stabilizing platform. The support is realized as follows: The horizontal position of the gyro-stabilized platform is controlled by two orthogonal horizontal accelerometers. The platform is leveled in such a manner that the horizontal accelerations are zero. If the ship describes a curve, the additional horizontal acceleration will cause the platform to be leveled according to the resulting apparent vertical axis. This axis may differ substantially from the true vertical axis and will result in reduced gravity values and additionally in an effect of horizontal accelerations on the measured gravity. The latter effect is eliminated by supplying the system with online navigation data. A microprocessor calculates the leveling errors from this input and enters them into the platform electronics which corrects the platform accordingly.

### 5.4.2 Gravity Ties to Land Stations

To compare the results of different gravity surveys the measured data have to be tied to a world-wide accepted reference system. This system is represented by the International Gravity Standardization Net IGSN71 (Morelli, 1974). The IGSN71 was established in 1971 by the International Union of Geodesy and Geophysics (IUGG) as a set of world-wide distributed locations with known absolute gravity values better than a few tenths of mGal. According to the

recommendations of the IUGG, every gravity survey, marine or land, should be related to the datum and the scale of the IGSN71.

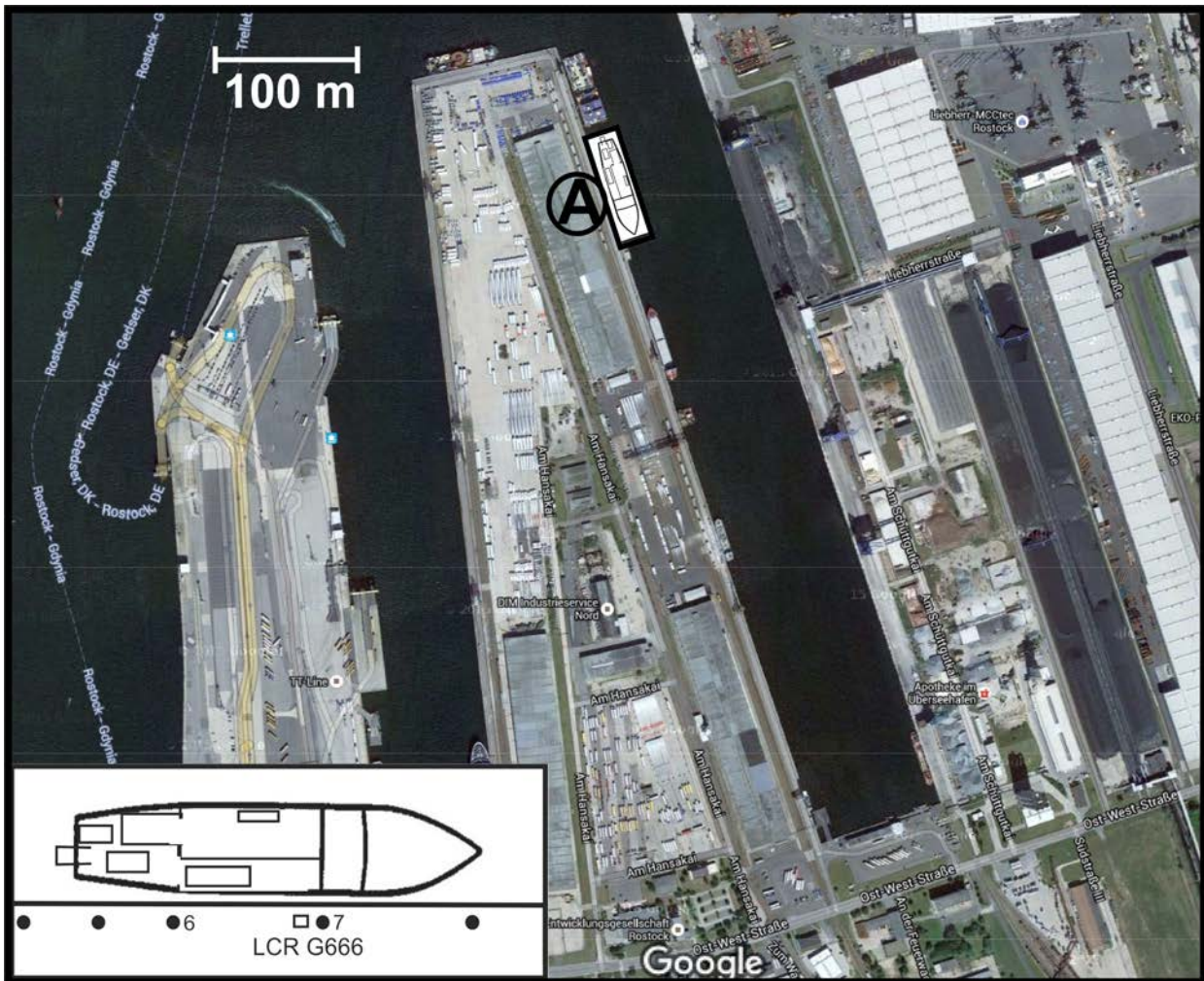


**Fig. 5.4.2.1** Location of the mooring site of RV MARIA S. MERIAN at the Hansakai in the Überseehafen of Rostock (A).

Therefore, gravity measurements on land have to be carried out to connect the gravity measurements at sea with the IGSN71. The marine geophysical group of BGR uses a LaCoste&Romberg gravity meter, model G, no. 666 (LCR G666) for the gravity connections. In Rostock a reference gravity station at the Warnemünde Church used (**01**). The point description and absolute gravity value of this station SFB183820110 was kindly provided by the Amt für Geoinformation, Vermessungs- und Katasterwesen Mecklenburg-Vorpommern. In Kiel a reference station at the Sartori Kai near the Schiffahrtsmuseum (**02**) was used. The description and absolute gravity value for this station 1626/8 was taken from the database of the Bureau de Gravimétrie International (BGI) in Toulouse.

For mobilization RV MARIA S. MERIAN moored at the Eastern Hansakai in the Überseehafen of Rostock about 165 m from the northern end of the pier (Fig. 5.4.2.1). On February 28, tie measurements to point **A** on the pier opposite the gravity room on RV MARIA S. MERIAN have been made. The connection measurements resulted in an average absolute gravity value of



981436.916 mGal (IGSN71, reduced to the gravity sensor level +1 m above the water level of 3.5 m) for point A. The reading of the KSS31M with the same water level on February 29 (8:00 UTC) was 539.18 mGal.

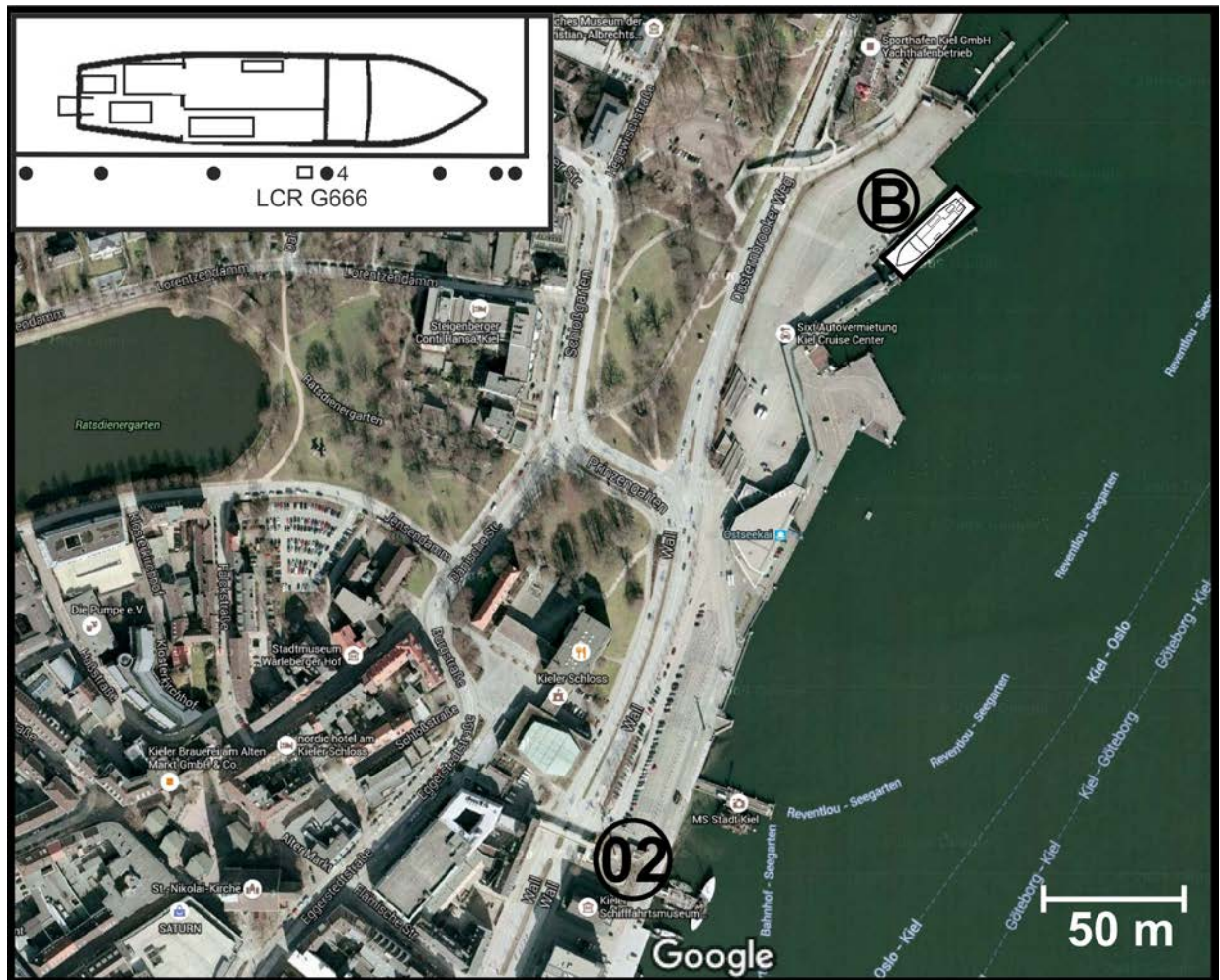


Fig. 5.4.2.2 Location of the mooring site of RV MARIA S. MERIAN at the Ostseekai in Kiel.

In Kiel RV MARIA S. MERIAN moored at the Ostseekai about 70 m from a south-western sharp kink of the pier (Fig. 5.4.2.2). On March 29, tie measurements to point B on the pier opposite the gravimeter room have been made. The connection measurements resulted in an average absolute gravity value of 981454.205 mGal (IGSN71, reduced to the gravity sensor level +1 m above the water level of 2.5 m) for point B. The reading of the KSS31M with the same water level after arrival on March 28, 11:20 UTC) was 555.45 mGal. The KSS31M readings in Rostock and Kiel imply an instrumental drift of -1.02 mGal in 27.2 days or -0.0375 mGal/day. This drift rate lies within the normal drift range of marine gravity measurements with the KSS31M. It was applied to the gravity data.

Station	Observer	Date	Time UTC	Reading units	Gravity value [mGal]
A	H	28.02.16	14:00	4955.88	5012.032
A	H	28.02.16	14:03	4955.87	5012.022
01	H	28.02.16	14:50	4958.53	5014.715
01	H	28.02.16	14:52	4958.54	5014.725
A	H	28.02.16	15:40	4955.72	5011.870
A	H	28.02.16	15:42	4955.74	5011.890
B	H	29.03.16	09:15	4973.05	5029.414
B	H	29.03.16	09:18	4973.03	5029.394
02	H	29.03.16	10:10	4972.50	5028.858
B	H	29.03.16	10:25	4973.00	5029.364
Observer: H = Heyde. Gravity in mGal using LCR G666 scaling table.					

**Table 5.4.2.1** Observation report of the gravity tie measurements in Rostock and Kiel.

**Reference Stations:**

01: Rostock-Warnemünde, Church, SFP 183820110 981439.018 mGal (IGSN71)  
 02: Kiel , Sartori Kai, No. 1626/8 981453.270 mGal (IGSN71)  
 (54°19.4'N, 10°08.6'E)

**Gravity stations:**

A: Rostock Überseehafen, Eastern Hansakai, 165 m from the northern end of the pier  
 B: Kiel, Ostseekai, 70 m from a south-western sharp kink of the pier

Differences between reference and gravity stations:

$$01 - A = 2.767 \text{ mGal}$$

Absolute gravity at A: 981436.251 mGal

Absolute gravity for A (reduced to sensor level -2.5 m): 981436.916 mGal (IGSN71 system)  
 used for the gravity tie on 29.02.2016 (08:00 UTC).

Reading of sea gravimeter KSS31 at that time: 539.18 mGal.

Difference between reference and gravity station:

$$02 - B = -0.536 \text{ mGal}$$

Absolute gravity at B: 981453.806 mGal

Absolute gravity for B (reduced to sensor level -1.5 m) 981454.205 mGal (IGSN71 system)  
 used for the gravity tie on 28.03.2016 (11:20 UTC).

Reading of sea gravimeter KSS31 at that time: 555.45 mGal.

### 5.4.3 Gravity data processing

Processing of the gravity data consists essentially of the following steps:

- a time shift of 76 seconds due to the overcritical damping of the sensor,
- conversion of the output from reading units (r.u.) to mGal by applying a conversion factor
- of 0.94542 mGal/r.u.. On this cruise this was done in the system itself by hardware settings
- connection of the harbour gravity value to the world gravity net IGSN 71,
- correction for the Eötvös effect using the navigation data,
- correction for the instrumental drift (not performed until completion of the cruise),
- subtraction of the normal gravity (WGS67).

As a result, we get the so-called free-air anomaly (FAA) which in the case of marine gravity is simply the Eötvös-corrected, observed absolute gravity minus the normal gravity. Gravity values were provided every second directly by the data handling subsystem of the KSS31M. The anomalies show at times short-wavelength oscillations in the order of 1-2 mGal especially during higher ship velocities. Therefore a median filter with a length of 180 s was applied to the data. Infrequent outliers were removed manually in advance. Additionally, data recorded during sharp turns and rapid speed changes of the vessel show disturbed values and were removed also manually.

## 5.5 Expected Results

### 5.5.1 Reflection Seismics

(C. Hübscher, N. V. Damm, M. Malinowski, V. Noack, M. Schnabel)

The suppression of surface multiples will be a challenging task during data processing due to the shallowness of the Baltic Sea. Methods based on velocity discrimination will not work properly for the 1<sup>st</sup> multiple since the move-out difference is not big enough and the number of traces or samples which are not deleted by nmo-stretch mute is too sparse. The probably most sophisticated method is the Surface Related Multiple Elimination (SRME) technique. It is quite costly in terms of processing time but known to be very effective. First test runs at the University of Hamburg after the cruise showed promising results (Fig. 5.5.1.1). The multiple is successfully suppressed without affecting primary reflections.

A W-E striking profile from the Bay of Kiel (Fig. 5.5.1.2) elucidates the structures of the Zechstein salt and the post-Permian succession (stratigraphy after Hansen et al., 2005). Crestal grabens emerged above two salt pillows. Upper Triassic strata are truncated by the Base Cretaceous which is a consequence of halokinetics during the Triassic West-East extension. Jurassic strata are missing; they were eroded during the North Sea dooming. The Cretaceous reveals a relatively constant thickness which implies a phase of reduced halokinetics. Halokinetics resumed in the late Tertiary. Where Tertiary strata are dissected by crestal graben faults tunnel valleys were eroded during the glacials. These valleys were filled after the retreat of the glaciers.

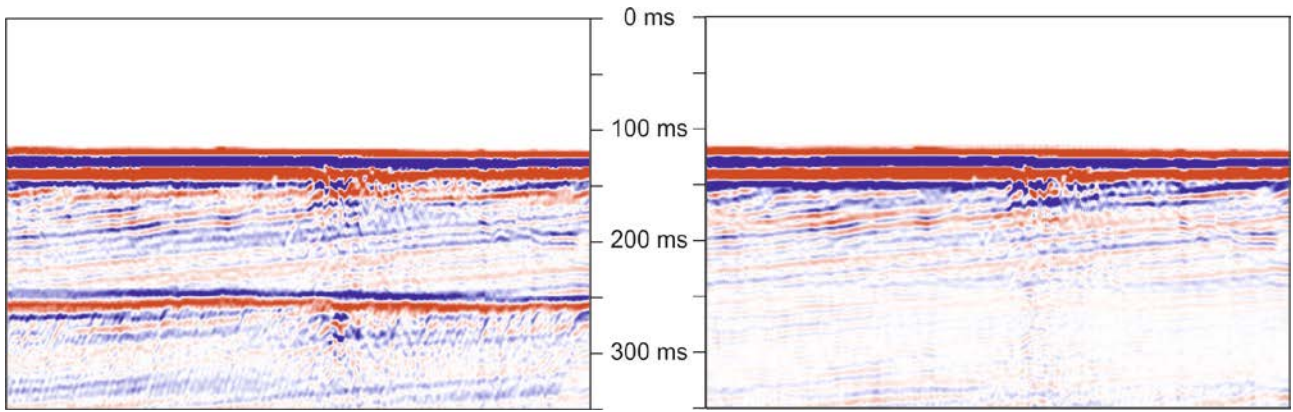


**Fig. 5.5.1.1** The strong water multiple cross-cuts and masks dipping reflections (left). After SRME processing previously masked reflections became visible (right).

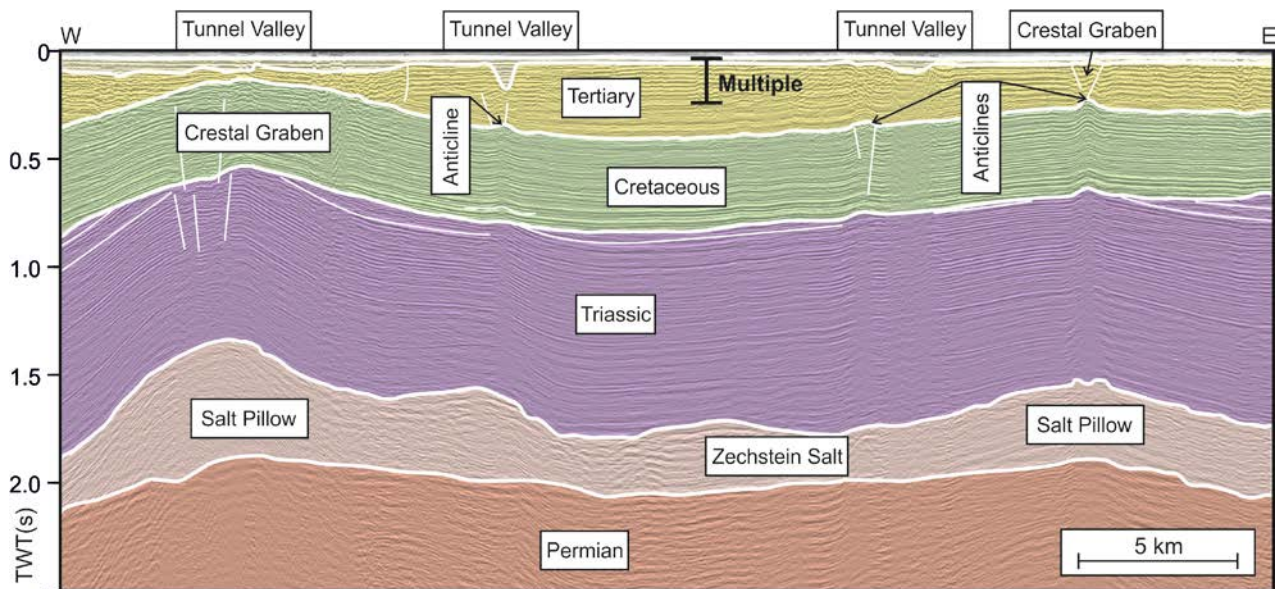


**Fig. 5.5.1.2** Interpreted seismic section from Bay of Kiel

Seismic data from the Bay of Mecklenburg reveal the same features (Fig. 5.5.1.3). A 3D-view illustrates the seismic profiles acquired in the Mecklenburg Bay (Fig. 5.5.1.4). According to both the processing flow and the high vertical penetration depth of the seismic data the base of the Zechstein salt is traceable on all profiles throughout the bays.

The data from the Bays of Kiel and Mecklenburg, both are part of the North German Basin, will help to understand in better detail the relationship between glacial erosion and halokinetics. So far, no subsalt fault could be imaged for the salt pillow in the Bay of Mecklenburg. We speculate that the salt pillow was formed during salt deposition as a consequence of basin subsidence (gravity gliding).

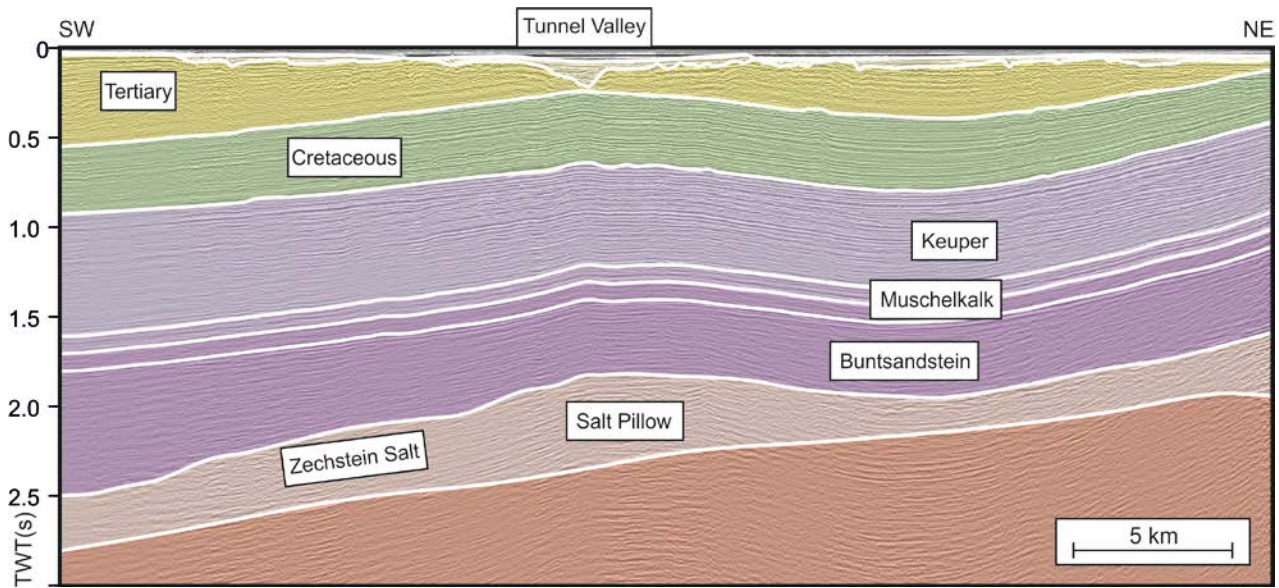


Fig. 5.5.1.3 Interpreted seismic section from Bay of Kiel

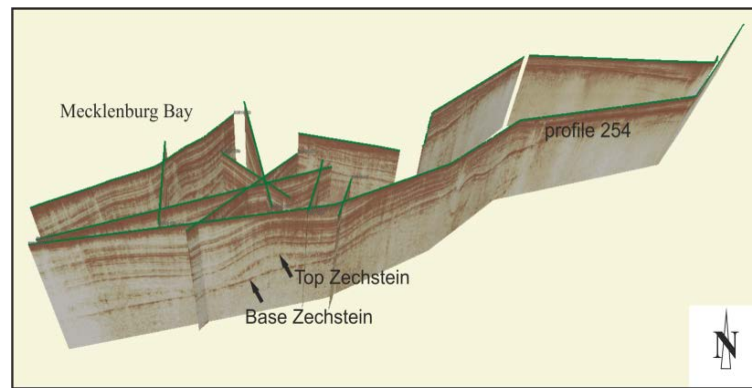


Fig. 5.5.1.4 3D-view of seismic sections collected in the Bay of Mecklenburg.

## 5.5.2 Streamer Refractions

(C. Hübscher, L. Frahm)

Due to the large streamer length compared to water depth the shot-gathers include refracted waves which appear as the first arrivals. These linear waves can be exploited in terms of layer thicknesses and layer velocities of the upper few hundred meters beneath sea floor. One data instance is shown in Fig. 5.5.2.1.

Those refraction and the guided waves are a problem both for velocity determination and imaging. A combination of  $f-k$  and  $Tau-p$  filtering turned out as an appropriate tool for suppressing those signals (Fig. 5.5.2.2).

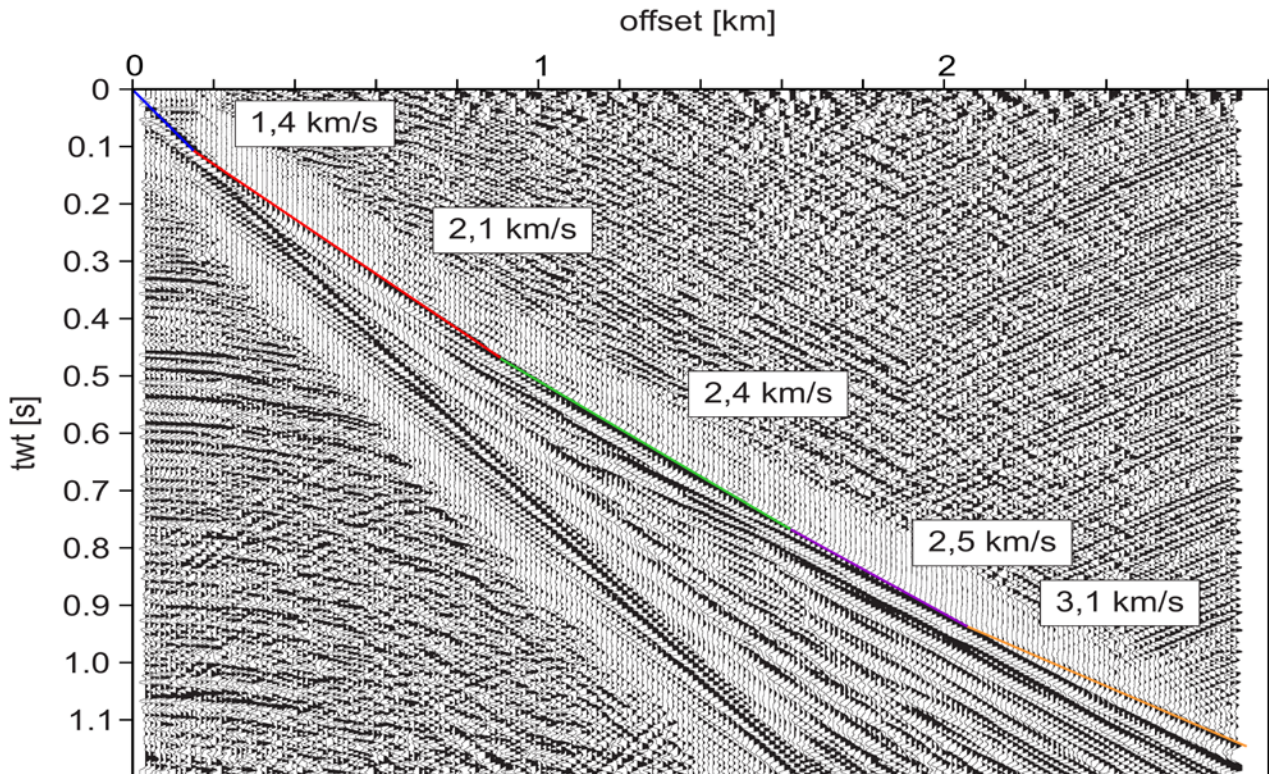


**Fig. 5.5.2.1** Shot-gather with refracted waves (colored lines) enhanced by and AGC of 200 ms. Numbers refer to apparent velocities.

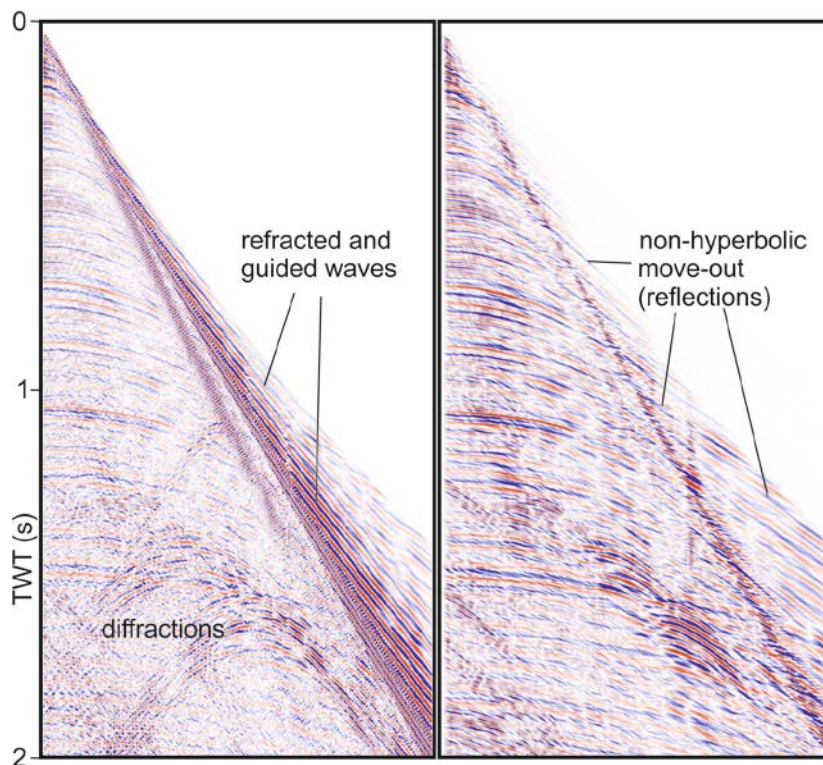


**Fig. 5.5.2.2** Shot-gather with refracted and guided waves (left). The non-hyperbolic far offset sector of reflections are visible after  $f$ - $k$  and  $Tau$ - $p$  filtering.

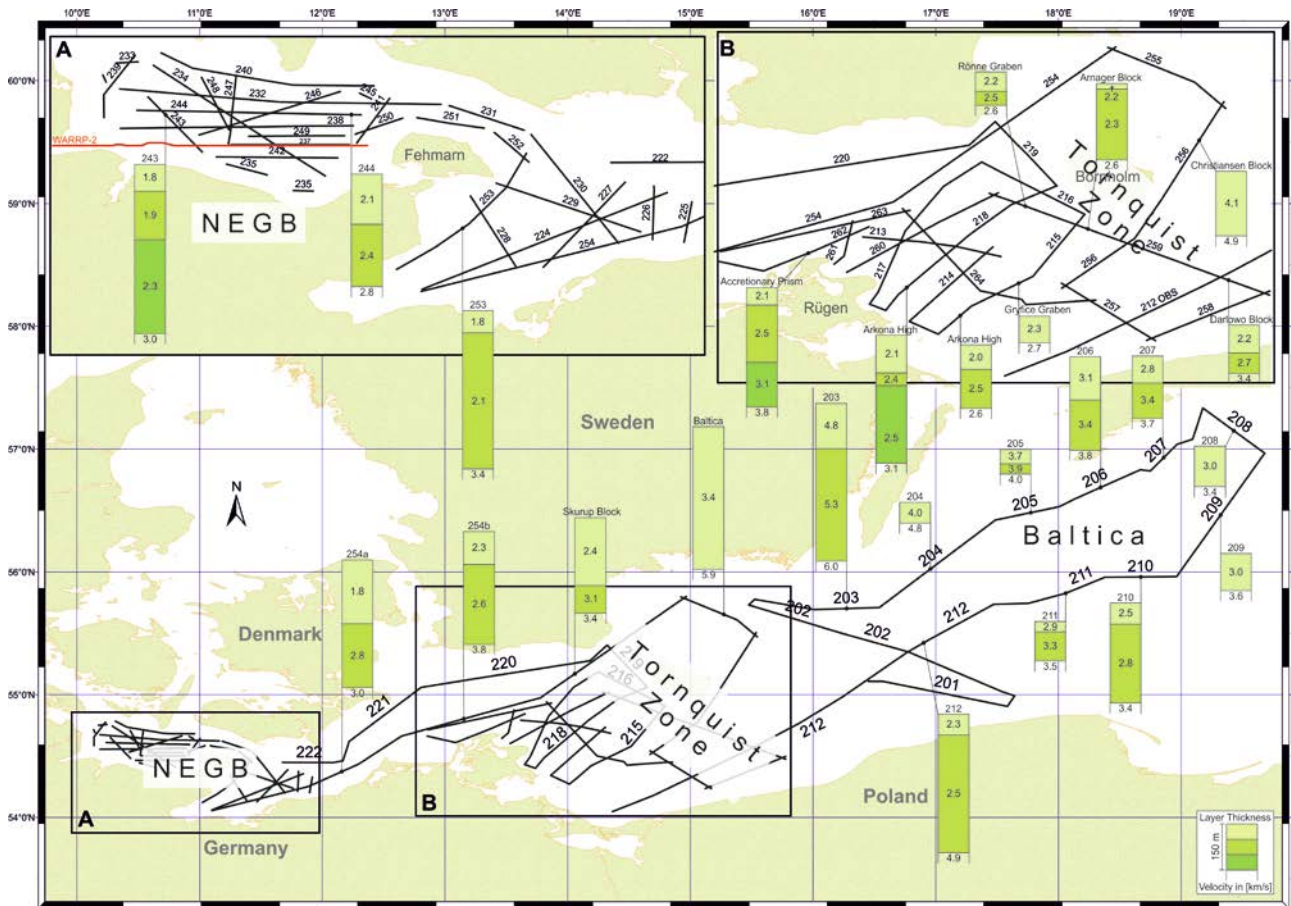


Fig. 5.5.2.3 Layer thicknesses and apparent velocities (instances).

Intercept times and apparent velocities have been used to derive velocity-depth models under the assumption of horizontal layering. We compared the calculated layer velocities with interval velocities which were derived from nmo-velocities (used as a proxy for  $V_{rms}$ ) by Dix inversion and stated a good agreement. Vice versa, the layer velocities derived from refracted waves were taken as a starting model for the reflection seismic processing.

Velocity-depth models are plotted in the map in Fig. 5.6.2.2. In the Bay of Kiel the upper few hundred meters comprising Cenozoic strata are characterized by velocities below 2.5 km/s. Paleozoic strata of the Baltic shield crop out beneath Quaternary strata in the north-eastern survey area and reveal velocities of  $> 5$ km/s.

### 5.5.3 OBS Recordings

(M. Malinowski)

The data quality along WARR profile 1 is variable, with better-quality records on the deeper water side (NE part of the line). In general, data quality from the broad-band Guralp nodes is much better than the short-period instruments. It is probably due to a better coupling of the seismometer and other technical differences (e.g. hydrophone mounting). Surprisingly, relatively small air-gun array (32 l) resulted in the data being recorded  $> 150$  km distance. Figs. 5.5.3.1-2 show example OBS gather, in which both crustal (Pg) and mantle phases (Pn, PmP) are present.

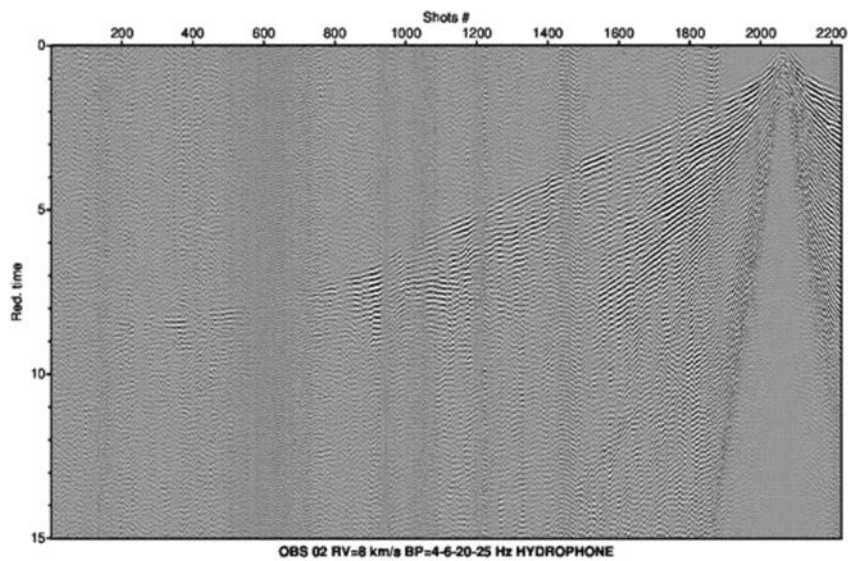


**Fig. 5.5.3.1** Example short-period Hamburg OBS gather from WARR1 (hydrophone channel). Reduction velocity of 8 km/s and band-pass filter of 4-6-20-25 Hz were applied.

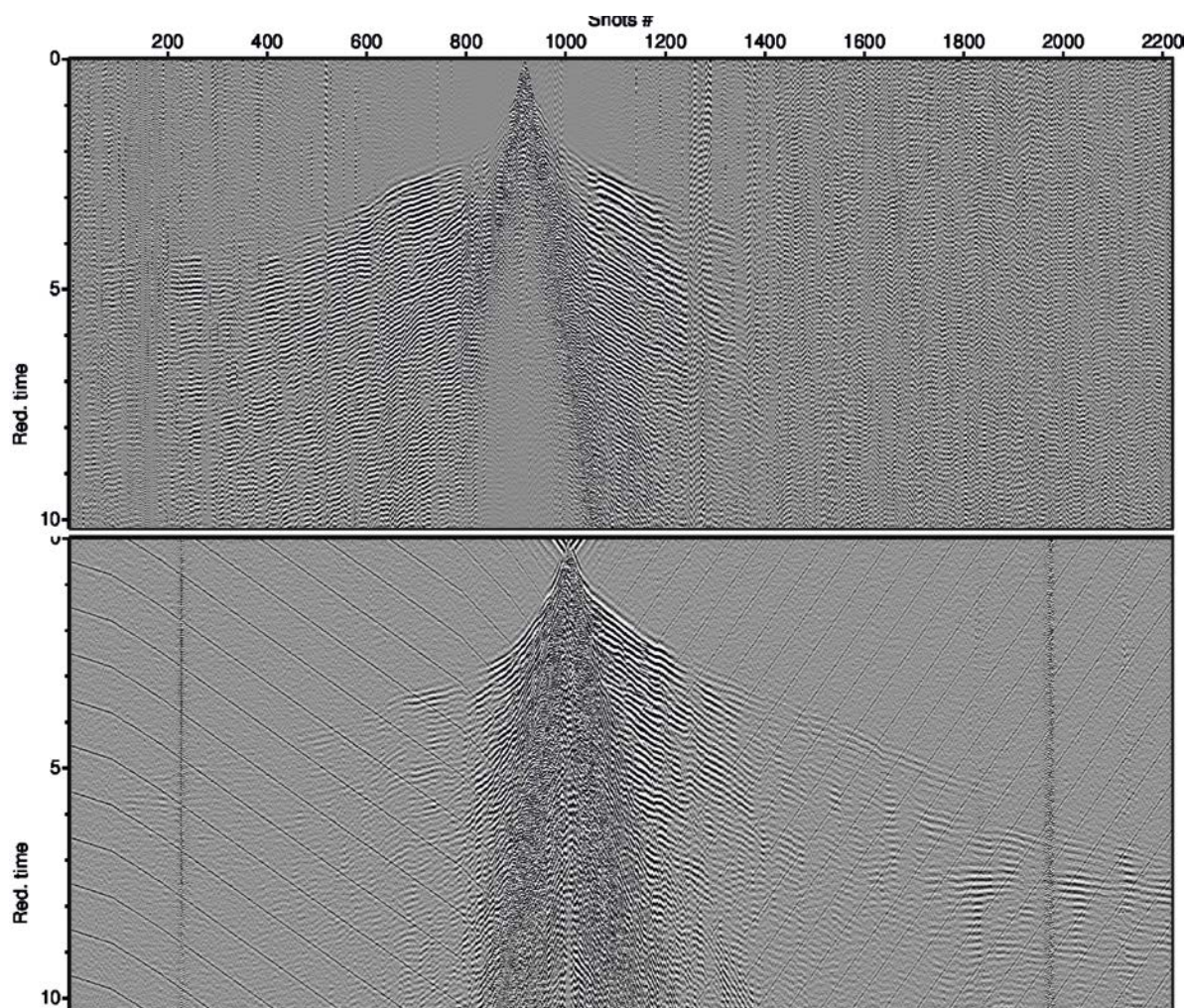


**Fig. 5.5.3.2** Comparison of the nearby OBS gathers from the short-period (top) and broad-band (bottom) nodes (profile WARR1). Plot of the vertical-component seismometer data. Reduction velocity of 8 km/s and band-pass filter of 4-6-20-25 Hz were applied.



### 5.5.4 Gravity Data

(I. Heyde, J. Bülow)

Gravity measurements were carried out continuously during the complete cruise (ca. 7000 km). Free air anomaly is plotted in Fig. 5.5.4.1.

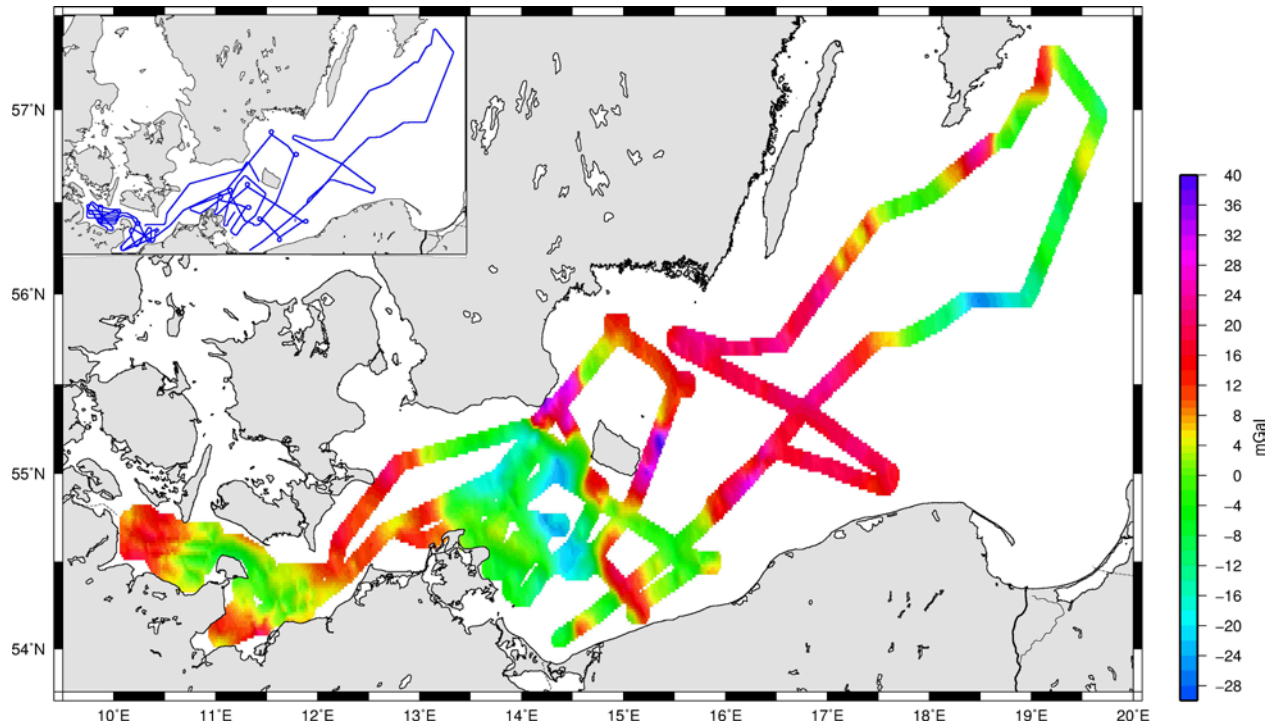


**Fig. 5.5.4.1** Map of the free-air gravity anomalies acquired during the profiles of cruise MSM52. The map is drawn up to a distance of 5 kilometers from the tracks. The map is based on a 1x1 (arc-) minutes grid. In the inset the MSM52 profiles with useful gravity measurements are shown.

Fig. 5.5.4.2 shows as an example the free-air gravity anomalies together with the bathymetry along profile BGR16-212 (for location see Fig. 3.3.1). The NE-SW running profile has a length of about 280 km and crosses the TTZ.

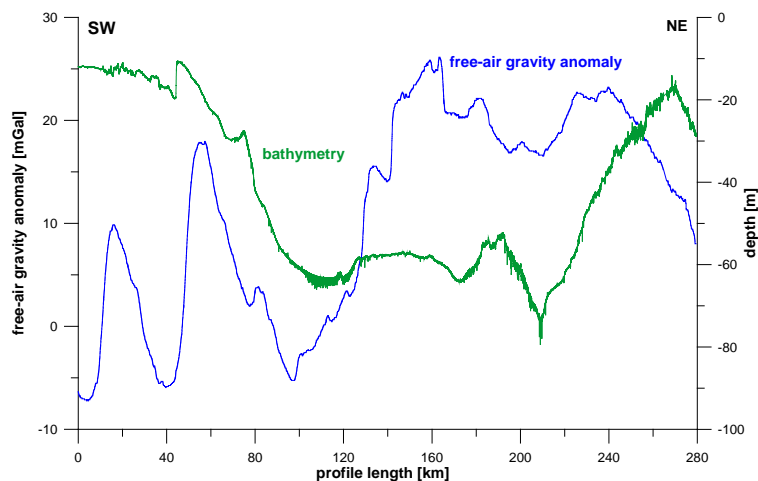


**Fig.5.5.4.2** Free-air gravity anomaly plotted against bathymetry of profile BGR16-212.

**6 Station List MSM52**

line number station number	shot point start/ end	date	time UTC	latitude	longitude	course	length (km)
BGR16-200d	1	02.03.16	18:39:00	54° 46.565 N	15° 51.250 E		
MSM52/105-1	2079	03.03.16	00:27:40	55° 6.599 N	16° 26.209 E	45°	52.52 km
BGR16-201	1	03.03.16	00:33:17	55° 6.855 N	16° 26.910 E		
MSM52/105-1	3346	03.03.16	09:50:47	55° 0.745 N	17° 36.359 E	98°	74.51 km
BGR16-202	1	03.03.16	09:51:40	55° 0.784 N	17° 36.248 E		
MSM52/105-1	5817	04.03.16	02:01:00	55° 43.415 N	15° 30.760 E	302°	153.84 km
BGR16-203	1	04.03.16	02:57:30	55° 46.433 N	15° 34.069 E		
MSM52/105-1	2363	04.03.16	09:31:10	55° 43.506 N	16° 32.920 E	95°	61.57 km
BGR16-204	1	04.03.16	09:32:10	55° 43.576 N	16° 33.015 E		
MSM52/105-1	3860	04.03.16	20:15:20	56° 25.783 N	17° 29.390 E	36°	97.47 km
BGR16-205	1	04.03.16	20:17:10	56° 25.849 N	17° 29.666 E		
MSM52/105-1	1202	04.03.16	23:37:20	56° 32.493 N	18° 0.443 E	68°	33.79 km
BGR16-206	1	04.03.16	23:40:10	56° 32.664 N	18° 0.797 E		
MSM52/105-1	1518	05.03.16	03:53:00	56° 47.372 N	18° 33.084 E	50°	42.67 km
BGR16-207a	1	05.03.16	05:23:50	56° 50.951 N	18° 45.800 E		
MSM52/105-1	868	05.03.16	07:52:20	57° 2.812 N	18° 57.801 E	29°	25.09 km
BGR16-207b	1	05.03.16	07:52:21	57° 2.813 N	18° 57.803 E		
MSM52/105-1	1840	05.03.16	11:34:12	57° 17.592 N	19° 14.355 E	31°	32.01 km
BGR16-208	1	05.03.16	11:36:27	57° 17.429 N	19° 14.585 E		
MSM52/105-1	1650	05.03.16	15:43:48	56° 59.396 N	19° 39.621 E	143°	41.81 km
BGR16-209	1	05.03.16	16:04:12	56° 57.626 N	19° 39.854 E		
MSM52/105-1	4695	06.03.16	03:48:18	55° 58.447 N	18° 56.202 E	202°	118.32 km
BGR16-210	1	06.03.16	03:50:06	55° 58.434 N	18° 55.906 E		
MSM52/105-1	1395	06.03.16	07:19:12	55° 57.781 N	18° 21.993 E	268°	35.16 km
BGR16-211	1	06.03.16	07:20:42	55° 57.706 N	18° 21.793 E		
MSM52/105-1	2350	06.03.16	13:13:03	55° 44.417 N	17° 27.654 E	247°	61.42 km
BGR16-212	1	06.03.16	13:15:00	55° 44.301 N	17° 27.388 E		
MSM52/105-1	11457	07.03.16	17:53:24	54° 3.288 N	14° 22.006 E	228°	271.89 km
BGR16-213	1	12.03.16	15:36:54	54° 48.726 N	13° 36.553 E		

MSM52/122-1	1905	12.03.16	20:22:30	54° 40.837 N	14° 19.148 E	107°	47.81 km
BGR16-214	1	12.03.16	21:54:54	54° 43.457 N	14° 17.223 E		
MSM52/122-1	1872	13.03.16	02:35:33	54° 22.006 N	13° 53.057 E	213°	47.45 km
BGR16-215a	1	13.03.16	04:10:03	54° 17.953 N	14° 2.426 E		
MSM52/122-1	3260	13.03.16	12:18:54	54° 53.632 N	14° 46.633 E	35°	81.32 km
BGR16-216	1	13.03.16	12:44:07	54° 55.692 N	14° 45.768 E		
MSM52/122-1	1598	13.03.16	16:43:48	55° 10.143 N	14° 17.142 E	312°	40.47 km
BGR16-217	1	13.03.16	17:12:00	55° 10.367 N	14° 13.098 E		
MSM52/122-1	3425	14.03.16	01:45:36	54° 28.070 N	13° 41.753 E	203°	85.16 km
BGR16-218	4040	14.03.16	03:17:51	54° 29.629 N	13° 48.654 E		
MSM52/122-1	7244	14.03.16	11:18:27	55° 3.156 N	14° 36.906 E	39°	80.68 km
BGR16-219	1	14.03.16	11:54:09	55° 6.091 N	14° 36.606 E		
MSM52/122-1	1320	14.03.16	15:12:00	55° 22.012 N	14° 21.322 E	331°	33.61 km
BGR16-220	1	14.03.16	15:46:30	55° 22.167 N	14° 16.639 E		
MSM52/122-1	3989	14.03.16	16:59:51	55° 16.684 N	14° 10.041 E	214°	12.30 km
BGR16-221	1	15.03.16	02:01:21	55° 2.721 N	12° 46.831 E		
MSM52/122-1	2950	15.03.16	09:23:42	54° 28.499 N	12° 10.420 E	212°	74.36 km
BGR16-222	146	15.03.16	10:07:03	54° 26.710 N	12° 5.001 E		
MSM52/122-1	1167	15.03.16	12:40:12	54° 26.733 N	11° 40.999 E	270°	25.84 km
BGR16-224	51	15.03.16	22:18:00	54° 3.823 N	11° 6.225 E		
MSM52/124-1	2325	16.03.16	03:59:06	54° 21.267 N	11° 50.418 E	56°	57.74 km
BGR16-225	150	16.03.16	06:19:03	54° 19.673 N	11° 54.946 E		
MSM52/124-1	645	16.03.16	07:33:18	54° 12.942 N	11° 53.654 E	186°	12.54 km
BGR16-226	65	16.03.16	08:44:33	54° 12.763 N	11° 47.713 E		
MSM52/124-1	766	16.03.16	10:29:42	54° 22.461 N	11° 48.040 E	1°	17.96 km
BGR16-227	109	16.03.16	11:23:15	54° 22.682 N	11° 42.352 E		
MSM52/124-1	1367	16.03.16	14:31:57	54° 7.627 N	11° 27.837 E	209°	32.00 km
BGR16-228	27	16.03.16	15:13:12	54° 7.974 N	11° 22.884 E		
	1026	16.03.16	17:43:03	54° 20.767 N	11° 14.573 E	339°	25.34 km
BGR16-229	198	16.03.16	18:33:09	54° 23.003 N	11° 19.357 E		
MSM52/124-1	532	16.03.16	19:23:15	54° 20.655 N	11° 26.002 E	121°	8.38 km

BGR16-229a	1	16.03.16	19:30:00	54° 20.352 N	11° 26.900 E		
MSM52/124-1	922	16.03.16	21:48:09	54° 14.087 N	11° 45.699 E	120°	23.40 km
BGR16-230	67	16.03.16	23:06:18	54° 12.794 N	11° 40.939 E		
MSM52/124-1	1598	17.03.16	02:55:57	54° 31.851 N	11° 25.692 E	335°	38.93 km
BGR16-231	1	17.03.16	03:06:28	54° 32.582 N	11° 24.599 E		
MSM52/124-1	643	17.03.16	04:42:45	54° 37.045 N	11° 10.870 E	299°	16.89 km
BGR16-232	13	17.03.16	04:54:18	54° 37.342 N	11° 9.098 E		
MSM52/124-1	2443	17.03.16	10:58:48	54° 40.114 N	10° 10.828 E	275°	62.64 km
BGR16-233	26	17.03.16	11:20:24	54° 41.298 N	10° 8.387 E		
MSM52/124-1	121	17.03.16	11:34:39	54° 42.545 N	10° 7.769 E	344°	2.40 km
BGR16-234	301	17.03.16	12:55:03	54° 44.301 N	10° 17.030 E		
MSM52/124-1	2264	17.03.16	17:49:30	54° 24.322 N	10° 48.188 E	138°	49.87 km
BGR16-235	211	17.03.16	18:33:18	54° 21.572 N	10° 45.965 E		
MSM52/124-1	1010	17.03.16	20:33:09	54° 26.411 N	10° 30.352 E	298°	19.07 km
BGR16-237	7	17.03.16	21:27:54	54° 29.983 N	10° 30.981 E		
MSM52/124-1	924	17.03.16	23:45:27	54° 29.991 N	10° 52.578 E	90°	23.22 km
BGR16-238	50	18.03.16	00:50:06	54° 33.457 N	10° 53.292 E		
MSM52/124-1	1845	18.03.16	05:19:21	54° 32.962 N	10° 10.988 E	269°	45.44 km
BGR16-239	10	18.03.16	05:52:57	54° 34.848 N	10° 7.904 E		
MSM52/124-1	895	18.03.16	08:05:42	54° 46.253 N	10° 13.618 E	16°	21.99 km
BGR16-240	1126	18.03.16	08:41:15	54° 46.704 N	10° 18.250 E		
MSM52/124-1	2871	18.03.16	13:03:00	54° 40.694 N	10° 57.057 E	105°	42.96 km
BGR16-241	40	18.03.16	13:43:21	54° 38.162 N	10° 59.756 E		
MSM52/124-1	713	18.03.16	15:24:18	54° 29.619 N	10° 53.599 E	203°	17.14 km
BGR16-242	17	18.03.16	15:58:12	54° 27.577 N	10° 50.606 E		
MSM52/124-1	967	18.03.16	18:20:42	54° 27.792 N	10° 28.272 E	271°	24.04 km
BGR16-243	25	18.03.16	18:40:03	54° 28.665 N	10° 25.824 E		
MSM52/124-1	865	18.03.16	20:46:03	54° 38.629 N	10° 15.974 E	330°	21.27 km
BGR16-244	23	18.03.16	22:04:12	54° 36.250 N	10° 13.800 E		
MSM52/124-1	1781	19.03.16	02:27:54	54° 35.425 N	10° 55.171 E	92°	44.41 km
BGR16-246	13	19.03.16	03:51:18	54° 39.619 N	10° 51.030 E		
MSM52/124-1	1250	19.03.16	06:56:51	54° 31.735 N	10° 25.188 E	242°	31.33 km

BGR16-247	134	21.03.16	17:48:09	54° 31.887 N	10° 30.826 E		
MSM52/137-1	940	21.03.16	19:49:03	54° 42.885 N	10° 31.993 E	4°	20.40 km
BGR16-248	1	21.03.16	20:55:39	54° 42.275 N	10° 25.652 E		
MSM52/137-1	889	21.03.16	23:08:51	54° 30.645 N	10° 31.748 E	163°	22.51 km
BGR16-249	17	22.03.16	01:17:51	54° 31.535 N	10° 34.237 E		
MSM52/137-1	815	22.03.16	03:17:33	54° 31.618 N	10° 51.660 E	89°	18.72 km
BGR16-250	14	22.03.16	03:31:39	54° 31.913 N	10° 53.575 E		
MSM52/137-1	435	22.03.16	04:34:48	54° 34.715 N	11° 2.246 E	61°	10.66 km
BGR16-251	14	22.03.16	04:52:12	54° 34.899 N	11° 4.841 E		
MSM52/137-1	530	22.03.16	06:09:36	54° 32.977 N	11° 16.998 E	105°	13.53 km
BGR16-252	4	22.03.16	06:24:45	54° 32.225 N	11° 19.004 E		
MSM52/137-1	461	22.03.16	07:33:18	54° 26.816 N	11° 25.257 E	146°	12.06 km
BGR16-253	2	22.03.16	09:15:00	54° 28.475 N	11° 24.831 E		
MSM52/137-1	1823	22.03.16	13:48:09	54° 7.259 N	11° 1.230 E	213°	46.84 km
BGR16-254	60	22.03.16	14:54:27	54° 3.236 N	11° 5.576 E		
MSM52/137-1	12208	23.03.16	21:16:39	55° 47.982 N	14° 57.322 E	50°	313.64 km
BGR16-255	43	23.03.16	22:57:18	55° 48.020 N	14° 54.772 E		
MSM52/137-1	2074	24.03.16	04:01:57	55° 28.946 N	15° 32.057 E	132°	52.59 km
BGR16-256	1	24.03.16	05:42:00	55° 30.527 N	15° 31.954 E		
MSM52/137-1	4775	24.03.16	17:38:06	54° 30.807 N	14° 39.619 E	207°	123.76 km
BGR16-257	25	24.03.16	19:06:18	54° 32.860 N	14° 40.110 E		
MSM52/137-1	1814	24.03.16	23:34:39	54° 14.510 N	15° 10.137 E	136°	46.93 km
BGR16-258	1	25.03.16	01:08:51	54° 14.635 N	15° 7.362 E		
MSM52/137-1	2045	25.03.16	06:15:27	54° 31.097 N	15° 48.368 E	55°	53.71 km
BGR16-259	35	25.03.16	07:39:00	54° 28.590 N	15° 47.666 E		
MSM52/137-1	4333	25.03.16	18:33:27	55° 1.674 N	14° 16.691 E	303°	114.91 km
BGR16-260	1	25.03.16	20:10:21	55° 1.378 N	14° 19.595 E		
MSM52/137-1	2630	26.03.16	02:44:42	54° 36.357 N	13° 31.695 E	228°	68.98 km
BGR16-261	33	26.03.16	03:41:33	54° 38.881 N	13° 27.638 E		
MSM52/137-1	1046	26.03.16	06:13:30	54° 52.608 N	13° 33.546 E	14°	26.19 km
BGR16-262	6	26.03.16	07:29:06	54° 50.799 N	13° 38.771 E		

MSM52/137-1	2286	26.03.16	13:11:06	54° 39.719 N	12° 51.104 E	248°	54.91 km
BGR16-263	53	26.03.16	13:55:57	54° 42.848 N	12° 51.328 E		
MSM52/137-1	2675	26.03.16	20:29:15	54° 56.027 N	13° 51.650 E	69°	68.82 km
BGR16-264	22	26.03.16	22:11:51	54° 56.686 N	13° 49.326 E		
MSM52/137-1	3543	27.03.16	07:00:00	54° 30.808 N	14° 43.665 E	129°	75.31 km
BGR16-2R1	1	10.03.16	01:55:00	54° 07.16 N	14° 31.35 E		
MSM52/122-1	705	10.03.16	07:47:00	54° 22.10 N	15° 01.35 E	49.5°	42.74 km
BGR16-R1a	1	10.03.16	07:48:00	54° 22.12 N	15°01.41 E		
MSM52/122-1	100	10.03.16	09:02:15	54° 25.34 N	15°07.43 E	46.3°	9.04 km
BGR16-R1b	1	10.03.16	09:04:00	54° 25.39 N	15° 07.52 E		
MSM52/122-1	1334	11.03.16	07:17:00	55° 24.40 N	16° 58.49 E	46.5°	161.39 km
BGR16-2R2	1	19.03.16	17:53:15	54° 33.24 N	10° 54.41		
MSM52/135-1	847	20.03.16	04:27:45	54° 29.32 N	9° 57.45	263.7 °	61.86 km
BGR16-2R3	1	20.03.16	04:28:30	54° 29.32 N	9° 57.45		
MSM52/135-1	663	20.03.16	12:45:34	54° 29.47 N	10° 54.48	89.2 °	61.61 km

## 7 Data and Sample Storage and Availability

All raw data acquired during the cruise will be copied and archived onboard using external drives. After the cruise, raw data will be synchronized with the professional long term archives of BGR (two separate mirrored data centers). Metadata will be published in the web accessible database systems PANGAEA (WDC-MARE) and the European database Geo-Seas. This allows users to contact the responsible scientists. The period of restricted data access will expire latest 2021. Bathymetric data will be delivered to the BSH data centre.

## 8 Acknowledgements

The MSM52 scientific party wishes to thank Master Ralf Schmidt and his crew for their outstanding support throughout the cruise. We are further grateful for the support of Control Station German Research Vessels, Briese-Research, the Federal Foreign Office and our embassies in Copenhagen, Stockholm and Warsaw.

## 9 References

- Abramovitz, T., Thybo, H., MONA LISA Working Group, 1998. Seismic structures across the Caledonian Deformation Front along MONA LISA profile 1 in the southeastern North Sea. *Tectonophysics* 288, 153-176.
- Al-Hseinat, M., Hübscher, C., 2014. Ice-load induced tectonics controlled tunnel valley evolution - instances from the southwestern Baltic. *Quaternary Science Reviews* 97, 121-135.
- Al-Hseinat, M., Hübscher, C., Lang, J., Lüdmann, T., Ott, T., Polom, U., 2016. Triassic to recent tectonic evolution of a crestal collapse graben above a salt-cored anticline in the Glückstadt Graben / North German Basin. *Tectonophysics* 680, 50-66.
- Baldschuhn, R., Binot, F., Fleig, S. & Kockel, F., 2001. Geotektonischer Atlas von Nordwest-Deutschland und dem deutschen Nordsee-Sektor. *Geol. Jb.*, A 153: 1–88.
- Berthelsen, A., 1992. Mobile Europe. In Blundell, D.J., Mueller, St and Freeman, R. (Eds.), *A continent revealed; The European Geotraverse project*. Cambridge University Press 11-32.
- Bertoni, C., Cartwright, J.A., 2006. Controls on the basinwide architecture of late Miocene (Messinian) evaporites on the Levant margin (Eastern Mediterranean). *Sedimentary Geology* 188-189, 93-114.
- Clausen, O. R., Pedersen, P. K., 1999. The Triassic structural evolution of the southern margin of the Ringkøbing-Fyn High, Denmark. *Marine and Petroleum Geology*, 16, 653-665.
- Cocks, LRM., McKerrow, WS., Van Staal, CR., 1997. The margin of Avalonia. *Geological Magazine* 134, 627-636.
- DEKORP-BASIN RESEARCH GROUP 1998. Survey provides seismic insights into an old suture zone. *EOS, Transactions*, 79(12): 151-159.
- Gradmann, S., Hübscher, C., Ben-Avraham, Z., Gajewski, D., Netzeband, G., 2005. Salt tectonic off northern Israel. *Marine and Petroleum Geology* 22(5), 597-611
- Gvirtzman, Z., Reshef, M., Buch-Leviatan, O., Ben-Avraham, Z., 2013. Intense salt deformation in the Levant Basin in the middle of the Messinian Salinity Crisis. *Earth and Planetary Science Letters* 379, 108-119.
- Hansen, M. B., Lykke-Andersen, H., Dehghani, A., Gajewski, D., Hübscher, C., Olesen, M., Reicherter, K., 2005. The Mesozoic–Cenozoic structural framework of the Bay of Kiel area, western Baltic Sea. *International Journal of Earth Sciences* 94, 1070-1082.
- Hübscher, C., Lykke-Andersen, H., Hansen, M.B., Reicherter, K., 2004. Investigating the Structural Evolution of the Western Baltic. *Transaction of the American Geophysical Union EOS* 85(12), 115.
- Hübscher, C., Borowski, C., 2006. Seismic evidence for fluid escape from Mesozoic cuesta type topography in the Skagerrak. *Marine and Petroleum Geology* 23, 17-28.
- Hübscher, C., Netzeband, G. 2007. Evolution of a young salt giant: The example of the Messinian evaporites in the Levantine Basin. In: Wallner, M., Lux, K.-H., Minkley, W., Hardy, Jr., H.R. (eds.) *The Mechanical Behaviour of Salt – Understanding of THMC Processes in Salt*. Taylor & Francis Group, London, ISBN 978-0-415-44398-2, pp.175-184.
- Hübscher, C., Dümmong, S., 2011. Levant Basin – Salt and fluid dynamic. In: Lofi *et al.*, Eds., *Atlas of Messinian seismic markers in the Mediterranean and Black seas*. *Mém. Soc. géol. fr.*, 179, and World Geological Map Commission, 72p.
- Hübscher, C., Hansen, M., Trinanes, S.P., Lykke-Anderson, H., Gajewski, D. 2010. Structure and evolution of the Northeastern German Basin and its transition onto the Baltic Shield. *Marine and Petroleum Geology* 27, 923-938.
- Kley, J., Voigt, T., 2008. Late Cretaceous intraplate thrusting in central Europe: Effect of Africa-Iberia-Europe convergence, not Alpine collision. *Geology* 36, 839-842.
- Kossow, D., Krawczyk, C., McCann, T., Strecker, M., Negendank, J.F.W., 2000. Style and evolution of salt pillows and related structures in the northern part of the Northeast German Basin. *International Journal of Earth Sciences*, 89, 652-664.
- Krawczyk, C.M., Eilts., F., Lassen, A., Thybo, H., 2002. Seismic evidence of Caledonian deformation crust and uppermost mantel structures in the northern part of the Trans-European Suture Zone, SW Baltic Sea. *Tectonophysics* 360, 215-244.
- Lang, J., Hampel, A., Brandes, C., Winsemann., 2014. Response of salt structures to ice-sheet loading: implications for ice-marginal and subglacial processes. *Quaternary Science Reviews* 101, 217-233.
- Maystrenko, Y., Bayer, U., Scheck-Wenderoth, M., 2005. The Glückstadt Graben, a sedimentary record between the North and Baltic Sea in north Central Europe. *Tectonophysics* 397, 113-126.
- Maystrenko, Y., Bayer, U., Brink, Scheck-Wenderoth, M., 2011. 3D structural model of the Glückstadt Graben, NW Germany Scientific Technical Report STR11/08 – Data. Potsdam, 29 pp.
- Mohr, M., Kukla, P.A., Urai, J.L., Bresser, G., 2005. Multiphase salt tectonic evolution in NW Germany: seismic interpretation and retro-deformation. *Int. J. of Earth Sci.* 94, 917-940.

- Mohr, M., Waren, J.K., Kukla, J.K., Urai, J.L., Irmen, A., 2007. Subsurface seismic record of salt glaciers in an extensional intracontinental setting (Late Triassic of NW Germany). *Geology* 35 (11), 963-966, [dx.doi.org/10.1130/G23378A.1](https://doi.org/10.1130/G23378A.1).
- Netzeband, G., Hübscher, C., Gajewski, D., 2006. The structural evolution of the Messinian Evaporites in the Levantine Basin. *Marine Geology* 230, 249-273.
- Obst, K., Deutschmann, A., Seidel, E., Meschede, M., 2015. Entwicklung eines 3D-Untergrundmodells für die südliche Ostsee – Grundlagen, Ziele und Ergebnisse des USO-Projektes. – 79. Tagung Norddeutscher Geologen, LUNG-Heft 1/2015, p. 118-121.
- Pharaoh, T.C., England, R.W., Verniers, J., Zelazniewicz, A., 1997. Introduction: geological and geophysical studies in the Trans-European Suture Zone. *Geological Magazine* 134, 585-590.
- Pharaoh, T.C., TESZ Colleagues., 1999. Trans-European Suture Zone. In Gee, D.G and Zeyen, H.J. (Eds.), EUROPROBE 1996- Lithosphere Dynamics: Origin and Evolution of Continents. 41-54, EUROPROBE Secretariate, Uppsala University.
- Reiche, S., Hübscher, C., Beitz, M., 2014. Fault-controlled evaporite deformation in the Levant Basin, Eastern Mediterranean. *Marine Geology* 354, 53-68.
- Reinhardt, H.-G. [Hrsg.] (1991): Regionales geophysikalisches Kartenwerk (1960 – 1991). – Unveröffentlichtes Kartenwerk, VEB Geophysik; Leipzig.
- Rempel, H., 1992. Erdölgeologische Bewertung der Arbeiten der gemeinsamen Organisation „Petrobaltic“ im deutschen Schelfbereich. – *Geologisches Jahrbuch*, Reihe D, p. 1-32; Hannover.
- Scheck, M., Bayer, U., 1999. Evolution of the Northeast German Basin – inferences from a 3D structural model and subsidence analysis. *Tectonophysics* 313, 145-169.
- Schlüter, H-U., Best, G., Jürgens, U., Binot, F. (1997): Interpretation reflexionsseismischer Profile zwischen baltischer Kontinentalplatte und kaledonischem Becken in der südlichen Ostsee – erste Ergebnisse. – *Zeitschrift der Deutschen Geologischen Gesellschaft* 148/1, p. 1-32.
- Sirocko, F., Reicherter, K., Lehne, R., Hübscher, Ch., Winsemann, J., Stackebrandt, W., 2008. Glaciation, salt and the present landscape (Chapter 4.5), In: Littke, R., Bayer, U., Gajewski, D., Nelskamp, S. (Eds.), *Dynamics of Complex Intercontinental Basins- The Central European Basin System*, Springer-Verlag, Berlin-Heidelberg, 519, 234-245.
- Thybo, H., 1997. Geophysical characteristics of the Tornquist Fan area, northwest Trans-European Suture Zone: indication of the late Carboniferous to early Permian dextral transtension. *Geological Magazine* 134(5), 597-606.
- Thybo, H., 2000. Crustal structure and tectonic evolution of the Tornquist Fan region as revealed by geophysical methods. *Bulletin of the Geological Society of Denmark* 46, 145-160.
- Thybo, H., Berthelsen, A., 1991. The Tornquist Zone and the Tornquist Fan. *Annales Geophysicae* 9 (suppl.), C21.
- Thybo, H., Pharaoh, T.C., Guterch, A., 1999. Geophysical investigations of the Trans-European Suture Zone. *Tectonophysics* 314(1-3), 161-174.
- Vendeville, B.C., Jackson, M.P.A., 1992. The rise of diapirs during thin-skinned extension. *Marine and Petroleum Geology* 9, 331-353.
- Warren, J.K., 2008. Salt as sediment in the Central European Basin system as seen from a deep time perspective. In: Littke, R., Bayer, U., Gajewski, D., Nelskamp, S. (Eds.), *Dynamics of Complex Intercontinental Basins- The Central European Basin System*, Springer-Verlag, Berlin-Heidelberg, 519, 249-276.
- Ziegler, P. A., 1990. *Geological Atlas of Western and Central Europe*. Shell International Petroleum Maatschappij Bv, distributed by Geological Society Publishing House, 239 pp.
- Zöllner, H., Reicherter, K., Schikowsky, P., 2008. High-resolution seismic analysis of the coastal Mecklenburg Bay (North German Basin): pre-Alpine evolution. *International Journal of Earth Sciences* DOI 10.1007/s00531-007-0277-9.



## 10 Appendix

### 10.1 Seismic Equipment and Survey Setup

(T. Behrens, V. Damm, Ü. Demir, M. Engels, B. Hahn, G. Lange, M. Schnabel)

#### Seismic sources

##### *Airgun system*

For the reflection seismic part of the survey we used GI-guns as seismic sources which allow getting a good vertical resolution of the uppermost structures at reasonable depth penetration. For the refraction seismic part of the survey we used G-guns which produce lower frequencies. In both cases a total number of 8 guns were used.

The airguns were mounted to two BGR owned hanger systems suitable for four guns in two clusters each (Fig. 10.1.1). All G-guns were provided by BGR, whereas half of the GI-guns were provided by both the University of Hamburg and BGR respectively.

The gun arrays were subdivided into two sub-arrays. Each sub-array consists of two clusters with two guns each. The individual volumes of the guns in the arrays were 250 in<sup>3</sup> for all G-guns and 45/105 in<sup>3</sup> for all GI-guns. The total volume of the starboard and portside arrays were 2000 in<sup>3</sup> for the G-gun and 1200 in<sup>3</sup> for the GI-gun sources.

In case of the reflection seismic survey operations we towed a hydrophone module of the QuietSea system which is designed for marine mammal detection and location. This AUX module was connected via a 10 m towing rope to the gun hangar resulting in a 7 m towing depth. For detail see Fig. 10.1.2. A small buoy was connected to the AUX module to give enough buoyancy.

The towing depth of the airguns was 6 m for the G gun clusters and 3 m for the GI gun clusters throughout the survey. Each sub-array has a total towing length of 25 m. The nominal working pressure of the guns was 2.400 psi (165 bar).

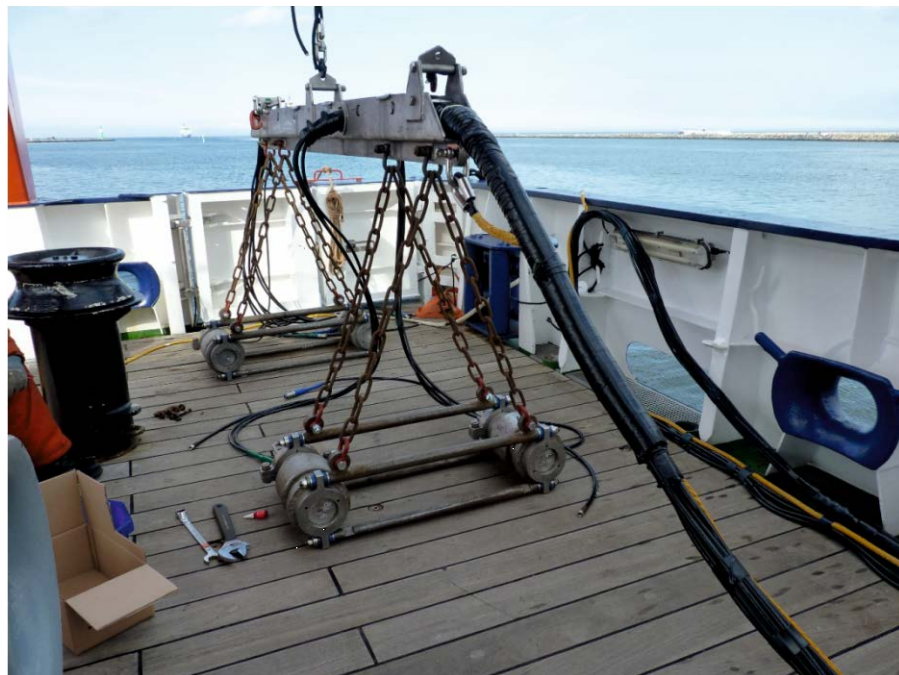


**Fig. 10.1.1** Portside gun hangar system.

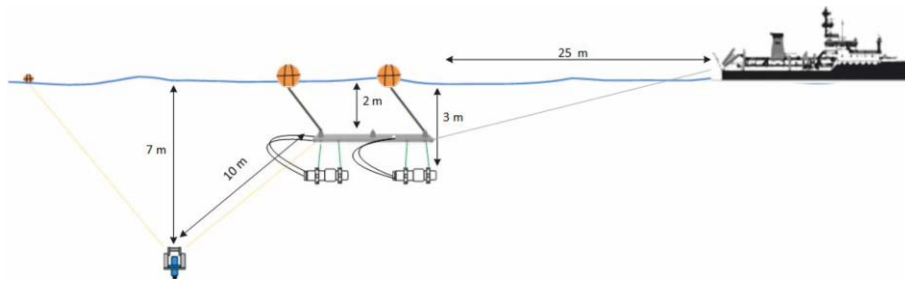


**Fig. 10.1.2** Airgun-system during cruise MSM52.

### Shot triggering

Before starting data acquisition a soft-start procedure of the airguns was completed. During this procedure we operated 4 minutes with one gun, shooting with an interval of 18 seconds. After 4 minutes a second gun was added and two guns together were shooting every 18 seconds. So each 4 Minutes one gun was added and after 24 minutes the soft-start procedure was finished. After that the regular shooting began for production of seismic lines.

#### *Shot triggering for multi-channel seismic profiling*

The shots were triggered in time intervals of 10 seconds for profiles BGR16-200a – BGR10-207, with 9 seconds for profiles BGR16-208 – BGR10-264.

#### *Shot Triggering for refraction seismic lines*

The shots for the refraction seismic experiment were triggered in time intervals of 30 seconds synchronized with GPS-Time over Meinberg GPS 170 interface card for profile BGR16-2R1, with 45 seconds for Profiles BGR16-2R1a, BGR16-2R2 and BGR16-2R3.


The shot time interval with the random function, representing an even distribution was generated on the Master PC with an interface card for triggering the airgun array via the SEAL428 system (see below) and the Syntron GCS 90 shot trigger device. The Master PC is running under Microsoft Windows XP and the Software is LabView Ver.8.6 from National Instruments.

### Seismic data acquisition

BGR's SEAL 428 seismic recording system and a digital cable with an active length of 2700 m (216 channels) were used to record the seismic data. The bird controlling system (DigiCOURSE System3) and the streamer control system are interfaced with the Master PC. The system start trigger was generated by Master PC. The data for the external header, e.g. from the DigiCOURSE, navigation system, GPS-clock etc., are received and the external header was generated, stored and sent via an interface to the SEAL system.

The SEAL 428 seismic recording system is a high-resolution seismic data acquisition system designed for marine towed streamers acquisition. The SEAL recording system is capable to handle a maximum recording capacity of 960 channels (@ 12.5 m; 2 ms) per streamer, a maximum record length of 47 s (navigation triggered, SR = 2 ms). The sampling rate may vary from 1/4 ms, 1/2 ms, 1 ms, 2 ms to 4 ms. During the cruise we sampled the data at 1 ms. The HP DL380 G7 Server is capable to support a maximum of 17500 channels (SR 2 ms).

**Fahrt: MSM 52 -BaITec 2016-**



Slip Ring		Lead In	SNS	HAU	SNS	RVIM	SNS	QS 50
10.6.210		405m/30m	70/70	0,28m	70/70	*17,5m	70/50	1
001		1045855129	5352069	1045855127	404006980	1043880160	6686779	

Flot CB1	Flot CB2	Flot CB3	Flot CB4	Flot CB5	Flot CB6
ALS 1	SNS	QS 50	ALS 2	SNS	QS 50
1 - 12	50/50	2	13 - 24	50/50	3
7018	1044624177	6686879	9251	1044624183	6686899

Flot CB7	Flot CB8	Flot CB9	Flot CB10	Flot CB11
ALS 3	SNS	QS 50	ALS 4	ALS 5
25 - 36	50/50	4	37 - 48	49 - 60
9256	1044624184	6687799	8637	9260

Flot CB7	Flot CB8	Flot CB9	Flot CB10	Flot CB11
ALS 9	ALS 10	LAUM	ALS 11	ALS 12
97 - 108	109 - 120	2	121 - 132	133 - 144
9252	9259	4017	9257	2175

Flot CB8	Flot CB9	Flot CB10	Flot CB11
ALS 13	ALS 14	ALS 15	LAUM
145 - 156	157 - 168	169 - 180	3
9237B	7027	9241	4373

Flot CB10	Flot CB11	Flot CB12	Flot CB13	Flot CB14
ALS 16	ALS 17	ALS 18	TAPU	TES
181 - 192	193 - 204	205 - 216	0,34m	50m
9253	9249	9248	867	3198

Unterfütterungen s. Fotos

Innere kurze Collar jeweils auf 5. Distanzstück hinter Headkupplung für zusätzl. Flotation Tubes

alle CB-Positionen sind mit QuickCuff-Collar bestückt

S/N von RVIM auf der Mutter kontrollieren!

bei Verwendung der kurzen Float die achterlichen inneren Collar umsetzen

Bird 1	S/N 60776
Bird 2	S/N 36192
Bird 3	S/N 36274
Bird 4	S/N 37995
Bird 5	S/N 58943
Bird 6	S/N 59524
Bird 7	S/N 59560
Bird 8	S/N 60644
Bird 9	S/N 60779
Bird 10	S/N 60782
Bird 11	S/N 60794

Ziehstumpf: Schleppauge 26 m von Tailkupplung + 4 m Draht

CB: Compassbird

Flot: Flotation Tube

RVIM: \* 19,5 m kalkulierte Länge, lastabhängig s. Tabelle

HAU: 0,28 m Länge


LAUM: 0,34 m Länge

SNS: 0,72 m Länge


QS 50: 0,27 m Länge

DR-Spule (grün): 9,3 m von Headkupplung

CB-Spule (blau): 140,6 m von Headkupplung



**Fahrt: MSM 52 -BaITec 2016-**



Slip Ring		Lead In	SNS	HAU	SNS	RVIM	SNS	QS 50
10.6.210		405m/30m	70/70	0,28m	70/70	*17,5m	70/50	1
001		1045855129	5352069	1045855127	404006980	1043880160	6686779	

Flot CB1	Flot CB2	Flot CB3	Flot CB4	Flot CB5	Flot CB6
ALS 1	SNS	QS 50	ALS 2	SNS	QS 50
1 - 12	50/50	2	13 - 24	50/50	3
9244	1044624177	6686879	9251	1044624183	6686899

Flot CB7	Flot CB8	Flot CB9	Flot CB10	Flot CB11
ALS 3	SNS	QS 50	ALS 4	ALS 5
25 - 36	50/50	4	37 - 48	49 - 60
9256	1044624184	6687799	8637	9260

Flot CB7	Flot CB8	Flot CB9	Flot CB10	Flot CB11
ALS 9	ALS 10	LAUM	ALS 11	ALS 12
97 - 108	109 - 120	2	121 - 132	133 - 144
9252	9259	4017	9257	2175

Flot CB8	Flot CB9	Flot CB10	Flot CB11
ALS 13	ALS 14	ALS 15	LAUM
145 - 156	157 - 168	169 - 180	3
9237B	7027	9241	4373

Flot CB10	Flot CB11	Flot CB12	Flot CB13	Flot CB14
ALS 16	ALS 17	ALS 18	TAPU	TES
181 - 192	193 - 204	205 - 216	0,34m	50m
9253	9249	9248	867	3198

Unterfütterungen s. Fotos

Innere kurze Collar jeweils auf 5. Distanzstück hinter Headkupplung für zusätzl. Flotation Tubes

alle CB-Positionen sind mit QuickCuff-Collar bestückt

S/N von RVIM auf der Mutter kontrollieren!

bei Verwendung der kurzen Float die achterlichen inneren Collar umsetzen

Bird 1	S/N 60776
Bird 2	S/N 36192
Bird 3	S/N 36274
Bird 4	S/N 37995
Bird 5	S/N 58943
Bird 6	S/N 59524
Bird 7	S/N 59560
Bird 8	S/N 60644
Bird 9	S/N 60779
Bird 10	S/N 60782
Bird 11	S/N 60794

Ziehstumpf: Schleppauge 26 m von Tailkupplung + 4 m Draht

CB: Compassbird

Flot: Flotation Tube

RVIM: \* 19,5 m kalkulierte Länge, lastabhängig s. Tabelle

HAU: 0,28 m Länge

LAUM: 0,34 m Länge

SNS: 0,72 m Länge

QS 50: 0,27 m Länge

DR-Spule (grün): 9,3 m von Headkupplung

CB-Spule (blau): 140,6 m von Headkupplung




Fig. 10.1.3 Streamer configuration used until March 21 (top) and from March 21 to March 27 (bottom).

The bird controlling system DigiCOURSE System 3 was used to control the vertical streamer position (depth) and to measure the heading and temperature. DigiCOURSE System 3 is a hardware and software package that controls and collects data from a network of acoustic sensors and streamer positioning devices. The system has online command, diagnostic, and performance-

monitoring capability. System 3 employs a modular architecture which provides for a variety of configurations and levels of functionality. The minimum system equipment configuration includes two real-time processors: an Operator Interface (OI) and a Data Management Unit (DMU), a Line Interface Unit (LIU), and cable-mounted measuring devices: birds with compass. It is suggested to get the full equipped streaming device self-buoyant. To produce more buoyancy we mounted at each bird position a floatation tube or instead of that a recovery system which has a self-triggering mechanism at a depth of 50 m. We operated the cable at a depth of 4 m.

BGR's SEAL digital streamer during cruise MSM52 consisted of 18 seismic sections (18\*ALS) with 216 channels (Figs. 10.1.3). It has a flexible architecture with redundant data transmission modes, i.e. data transmission may be reconfigured on line failure. Each channel has an individual 24 bit, Sigma Delta A/D converter. The active streamer sections have a diameter of 50 mm.

### **In-water equipment modules**

The seismic data are amplified, filtered, and analogue-digital converted within the SEAL streamer by using the following main modules installed in the streamer:

4 LAUM-428, 1 TAPU, 1 AXCUC and 1 HAU 428.

**Lead In**                    The Lead In is an armoured towing cable and tows the seismic cable. The cable contains an electric core for power transmission and four optical fibers for data transmission (two used, two spare).

**RVIM**                    Radial Vibration Isolation Module. RVIM is used to isolate vessel, handling equipment, and tow-leader mechanical vibration from the active cable.

**SHS**                    Short Head Section. The SHS adapts mechanical the Lead-In and the streamer.

**HESA**                    Head Elastic Section Adapter. The HESA adapt the connectors between the HESE (70 mm connector) and the active part of the streamer (50 mm connector). This includes also two Water Break hydrophones at 0.38 m and 1.07 m measured from the front.

**HAU 428**                Head Auxiliary Unit 428. The HAU428 provide power to telemetry lines, provide power to the TLFOI (Tail Lead-In Fiber Optic Interface) and measures the tension on the streamer.

**ALS**                    Acquisition Liquid Section. Our Streamer was composed of 24 ALS. The Acquisition Liquid Section is filled with Isopar. To reduce fluid movement, oil block bulkheads are mounted on either side of every channel. The active sections hold the electronics for the seismic acquisition. It also contains depth bird and acoustic positioning coils. An active section is 150m long and contains six Field Digitizer Units (FDU2M) to acquire and digitize 12 channels. A channel is composed of a group of 16 hydrophones, the space between two channels is 12.5m.

**LAUM**                    Line Acquisition Unit Marine. The LAUM performs data routing, power supply of max. 60 active channels, decimating, filtering and compressing on the data before sending it back to the DCXU 428. It also synchronise all the samples with the time break.

**TAPU**                    Tail Acquisition and Power Unit. The TAPU includes the same functions as the LAUM. It performs also supplying 40 V<sub>DC</sub>, 30 W power to the tail buoy and re-routing of the data if needed.

**TES** Tail Elastic Stretch. The TES is used as mechanical and noise uncoupling between the active part of the streamer and the tail equipment (e.g. tail buoy).

**STIC** Streamer to Tail Interface Cable. The STIC interface between streamer and tail buoy.

### **Onboard equipment modules**

**SERVER 428** The server computer we used is a “HP DL380 G7”. The software is based on the Linux distribution RedHat version 6.3 ES 64 bit. The HP DL380 G7 Server is capable to support a maximum of 17500 channels (SR 2 ms). The Server is used for formatting the 24 bit data from the streamer interfaces and auxiliary interfaces into IEEE standard and then to SEG-D. The server manages the export process to the external storage devices (NAS), the e-SQC Pro system and the QuietSea system.

**CLIENT 428** The workstation we used is a HP Z420 computer. The software is based on the Linux distribution RedHat version 6.3 ES 64 bit. The client computer is used for user interaction with the SEAL 428 system. The operator controls the complete SEAL 428 system through the client computer.

**LCI 428** Line Control Unit 428. The LCI 428 detect the T0 pulse from navigation, retrieve the navigation header by serial link and retrieve data from the AXCUs auxiliary channels.

**DCXU 428** Deck Cable Crossing Unit 428. The DCXU-428 is used as an interface between the streamer and the server. It also houses a high-voltage power supply for the streamer’s electronic. The DCXU 428 is also used as an interface between the streamer and the bird controller and QuietSea system.

**Time Server** The “Meinberg LanTime M300” Time server is disciplined by GPS and/or GLONASS satellites and provides a time base with an accuracy of  $10^{-13}$  sec. The time server provides all the necessary signals to ensure the synchronisation of all SEAL components. A PPS signal and a NMEA frame synchronize all the DCXU 428 and LCI 428 and a NTP network protocol synchronizes the server and client computers.

**AXCU** Auxiliary Channel Unit. The AXCUs are able to sample any analog signal. The AXCUs were used to record the signature from the GI-Guns.

**NAS** We used two external storages (QNAP TS-569 Pro and TS-259 Pro+) for the produced SEG-D files.

### **eSQC-Pro Processing Quality Control**

Continuous online seismic data quality control is performed using an eSQC-Pro client ‘HP Z420’ connected directly to the eSQC-Pro Server “HP DL380” without slowing down the acquisition. Three main windows are used for quality control:

- The History display window with bar graphs shows a summary of errors and source attributes for the successive shots processed by the eSQC-Pro. It displays the attributes of the data from the previous shots.

- The Normal display window shows the latest incoming SEG-D shot record. The traces are displayed in the time/distance range with the noise of each trace on top of the display.

- The Single Trace window shows the data of one selected channel from the streamer. With each new shot the display is updated with the new acquired trace added to the window. Four single trace windows may be opened simultaneously.